# Abstract

Delivery of nucleic acid is a promising approach for genetic diseases/disorders. However, gene therapy using oligonucleotides (ONs) suffers from low transfection efficacy due to negative charges, weak cellular permeability, and enzymatic degradation. Thus, cell-penetrating peptide (CPP), is a short cationic peptide, is used to improve the cell transfection. In this thesis, new strategies for gene transfection using the CPP vectors in complex with ONs without and with nanoparticles, such as magnetic nanoparticles (MNPs, $Fe_3O_4$), and graphene oxide (GO), are investigated. Furthermore, the possible CPP uptake signalling pathways are also discussed.

A fragment quantitative structure-activity relationship (FQSAR) model is applied to predict new effective peptides for plasmid DNA transfection. The best-predicted peptides were able to transfect plasmids with significant enhancement compared to the other peptides. CPPs (PeptFect220 (denoted PF220), PF221, PF222, PF223, PF224) generated from the FQSAR, and standard PF14 were able to form self-assembled complexes with MNPs and GO. The formed new hybrid vectors improved the cell transfection for plasmid (pGL3), splicing correcting oligonucleotides (SCO), and small interfering RNA (siRNA). These vectors showed high cell biocompatibility and offered high transfection efficiency (> 4-fold for MNPs, 10–25-fold for GO) compared to PF14/SCO complex, which was before reported with a higher efficacy compared to the commercial lipid-based transfection vector Lipofectamine™2000. The high transfection efficiency of the novel complexes (CPP/ON/MNPs and CPP/ON/GO) may be due to their low cytotoxicity, and the synergistic effect of MNPs, GO, and CPPs. In vivo gene delivery using PF14/pDNA/MNPs was also reported. The assembly of CPPs/ON with MNPs or GO is promising and may open new venues for potent and selective gene therapy using external stimuli. The uptake signaling pathways using CPPs vectors, the RNA expression profile for PF14, with and without ON were investigated using RNA sequencing and qPCR analysis. Data showed that the signaling pathways are due to the regulation of autophagy-related genes. Our study revealed that the autophagy regulating proteins are concentration-dependent. Confocal microscopy and transmission electron microscopy have demonstrated the autophagy initiation and colocalization of ON with autophagosomes. Results showed that the cellular uptake of CPP-based transfection activates the autophagy signaling pathway. These findings may open new opportunities to use autophagy modifiers in gene therapy.

# Populärvetenskaplig Sammanfattning

Genterapi med hjälp av av oligonukleotider (ON) har en enorm potential för behandling av olika genetiska sjukdomar. För att ha terapeutisk effekt måste dock oligonukleotiderna nå in i cellen och detta försvåras på grund av deras negativa laddningar och snabba nedbrytning. Cellpenetrerande peptider (CPP), är korta katjoniska peptider, som kan användas för att förbättra det cellulära upptaget (transfektionen) av oligonukleotider. I denna avhandling undersöks nya strategier för hur CPP tillsammans med magnetiska nanopartiklar, såsom MNP och Fe3O4, eller grafenoxid (GO) nanopartiklar, kan möjliggöra effektivare transfektion av ON. Vidare studeras även de möjliga cellulära signalvägar som reglerar CPP-medierat upptag.

En så kallad ”fragment quantitative structure-activity relationship” (FQSAR) modell användes för att förutsäga nya effektiva CPP för leverans av plasmider (ringformade DNA-molekyler med omkring 5000 nukleotidbaspar). De bäst prediktade peptiderna visade en signifikant ökad transfektionsförmåga jämfört med den tidigare använda peptiden PeptFect 14 (PF14). De nya peptiderna PF220, PF221, PF222, PF223 och PF224 som identifierades med FQSAR kunde dessutom bilda självmonterande komplex med MNP eller GO nanopartiklar. I cellulära försök uppvisade dessa nya hybridvektorer (CPP/MNP och CPP/GO) en klart förbättrad transfektionsförmåga av såväl plasmider, som splitsningskorrigerande oligonukleotider (SCO) och små interfererande RNA (siRNA), jämfört med PF14-nanopartikel hybridvektorer, såväl som den kommersiella lipidbaserade transfektionsvektorn Lipofectamine™ 2000. Den höga transfektionseffektiviteten hos dessa nya hybridvektorer beror troligen på deras låga cellulära toxicitet och en möjlig synergistisk effekt vid kombinationen av CPP och MNP/GO nanopartiklar. Förmågan hos en CPP/MNP hybridvektor att levera plasmider in vivo undersöktes också och transfektion av celler i såväl lunga och mjälte i behandlade djur kunde påvisas. Dessa nya hybridvektorer utgör således en ny lovande strategi för leverans av ON vid genterapi. För att kartlägga de signalvägar som kontrollerar upptaget av CPP-baserade vektorer analyserades genuttrycket hos celler som transfekterats med PF14 eller PF14-ON, med hjälp av RNA-sekvensering och qPCR-analys. Resultaten påvisade att en ökning i uttrycket av flera autofagirelaterade gener sker tidigt vid transfektionen. Konfokal- och transmissionselektronmikroskopi demonstrerade vidare en ökad initiering av autofagi och samlokalisering av ON med autofagosomer. Detta visar att CPP-medierad transfektion aktiverar signalvägar som stryr autofagi och öppnar nya möjligheter att använda autofagimodifierare för att förbättra genterapi.

# List of publications

This thesis is based on the articles below:

I. **M. Dowaidar,** J. Regberg, D. A Dobchev, T. Lehto, M. Hällbrink, M. Karelson, Ü. Langel (2017) Refinement of a Quantitative Structure–Activity Relationship Model for Prediction of Cell-Penetrating Peptide Based Transfection Systems. Int J Pept Res Ther 23:91–100. doi: 10.1007/s10989-016-9542-8

**My Contribution**: I performed the leading role in the investigation. I conceived, designed, and guided the project. I did the synthesis and characterization of the CPPs, analyzed the data and wrote the manuscript.

II. **M. Dowaidar,** H. N. Abdelhamid, M. Hällbrink, K. Freimann, K. Kurrikoff, X. Zou, Ü. Langel (2017) Magnetic Nanoparticle Assisted Self-assembly of Cell Penetrating Peptides-Oligonucleotides Complexes for Gene Delivery. Scientific Reports, 7:9159. doi: 10.1038/s41598-017-09803-z.

**My Contribution**: I performed the leading role in the investigation. I did the synthesis of the CPPs, tested the biological activity, analyzed the data and participate in the writing of the manuscript.

III. **M. Dowaidar,** H. N. Abdelhamid, M. Hällbrink, X. Zou, Ü. Langel (2017) Graphene oxide nanosheets in complex with cell penetrating peptides for oligonucleotides delivery. Biochim Biophys Acta - Gen Subj 1861:2334–2341. doi: 10.1016/j.bbagen.2017.07.002

**My Contribution**: I performed the leading role in the investigation. I performed the synthesis of the CPPs, tested the biological activity, analyzed the data and participate in the writing of the manuscript.

IV. **M. Dowaidar,** M. Gestin, C. Pasquale Cerrato, M. H. Jafferali, H. Margus, P. Kivistik, K. Ezzat, E. Hallberg, M. Pooga, M. Hällbrink, Ü. Langel (2017) Role of autophagy in cell-penetrating peptide transfection model. Scientific Reports, *7*(1). doi:10.1038/s41598-017-12747-z

**My Contribution**: I performed the leading role in the investigation. I performed the synthesis of the CPPs, tested the biological activity, analyzed the data and wrote the manuscript.

# Abbreviations

| | |
|---|---|
| AMBER | Assisted Model Building with Energy Refinement |
| AMBRA1 | Activating molecule in Beclin-1 regulated autophagy 1 |
| ATP | Adenosine triphosphate |
| Chon | Chondroitin sulfate |
| CMA | Chaperone-mediated autophagy |
| CPP | Cell-penetrating peptide |
| CQ | Chloroquine |
| Dex | Dextran sulfate |
| DLS | Dynamic light scattering |
| EM | Electron microscopy |
| Fmoc | 9-fluorenylmethyloxycarbonyl |
| FQSAR | Fragment quantitative structure-activity relationship |
| Fuc | Fucoidin |
| GABARAP | GABA type A receptor-associated protein |
| Gal | Galactose |
| GFP | Green fluorescent protein |
| GO | Graphene oxide |
| GO-LCO GO | functionalized lactosylated chitosan oligosaccharide |
| HCQ | Hydroxychloroquine |
| HEK-293 | Human embryonic kidney |
| HIV-1 | Human immunodeficiency virus-1 |
| hMSCs | Human mesenchymal stem cells |
| HPLC | Reversed-phase high-performance liquid chromatography |
| MALDI-TOF-MS | Matrix-assisted laser desorption/ionization - time of flight mass spectrometry |
| MAP | Model amphipathic peptide |
| MAP1LC3 | Microtubule-Associated Protein 1 Light Chain 3 |
| MNPs | $Fe_3O_4$ magnetic nanoparticles |
| mTOR | Mammalian target of rapamycin |
| NLS | Nuclear localization sequence |
| ON | Oligonucleotide |
| PAMAM | Polyamidoamine |

| | |
|---|---|
| PCS | Photon correlation spectroscopy |
| PDMAEMA | Poly(2-dimethylaminoethyl methacrylate) |
| pDNA | Plasmid DNA |
| PE | Phosphatidylethanolamine |
| PEG | Polyethylene glycol |
| PEI | Polyethyleneimine |
| Poly C | Polycytidylic acid |
| Poly I | Polyinosinic acid |
| PPI | Polypropylenimine |
| QSAR | Quantitative structure-activity relationship models |
| RES | Reticular endothelial system |
| rGO | Reduced graphene oxide |
| SCARA | Scavenger class A |
| SCO | Splicing correcting oligonucleotides |
| SEM | Scanning electron microscopy |
| siRNA | Small interfering RNA |
| SPIONs | Superparamagnetic iron oxide nanoparticles |
| SPPS | Solid-phase peptide synthesis |
| SWCNTs | Single-walled carbon nanotubes |
| TAT | Transacting activator of transcription |
| TEM | Transmission electron microscopy |
| TFA | Trifluoroacetic acid |
| TIS | Triisopropylsilane |
| TRUS | Transrectal ultrasound |
| UVRAG | Ultraviolet irradiation resistant-associated gene |
| ζ potential | zeta potential |

# Contents

# 1. Introduction

## 1.1. Oligonucleotide delivery

Oligonucleotide (ON) delivery to mammalian cells has been considered as a leading research area for modern molecular biology and biotechnology[1]. The last decades showed advanced progress in human genome research and ON delivery for *in vitro* and *in vivo* studies. The early studies successfully showed uptake and expression of exogenous DNA into mammalian cells, and investigators used this strategy in gene therapy development for the treatment of several human disorders. The general concept of gene therapy includes transfecting nucleic acid to repair the missing or mutated nucleic acid and correct or adjust endogenous gene expression. Gene therapy can be used to treat genetic diseases, such as Duchenne muscular dystrophy and adenosine deaminase deficiency and disorders (e.g., cancer). However, there are still significant barriers that should be overcomed[2,3].

Oligonucleotide delivery lacks specificity and faces metabolic degradation by nucleases[2,4]. Therefore, it is necessary to evolve the safe ON delivery methods with potent targeting moieties and enhance its transfection efficacy. Thus, viral vectors or non-viral vectors were investigated as a carrier for oligonucleotides[5] (Figure 1).

## 1.2. Viral vectors

Viral vectors offer an effective method for transfection of ONs. However, they lack high safety. In all cases, targeting the tissue of interest still needs enhancement. In a model of improving gene therapy specificity, cells can be transfected ex-vivo as in the state of Strimvelis (Figure 2).

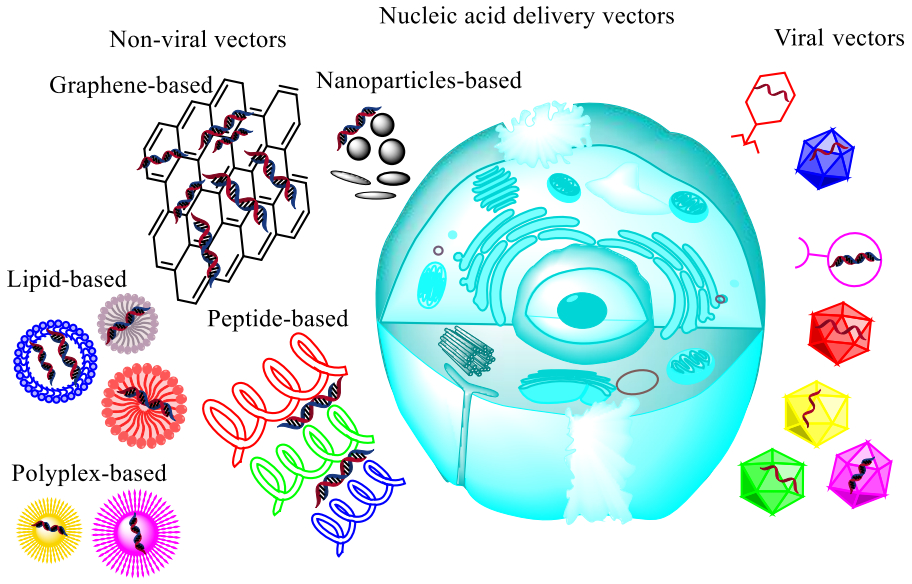


*Figure 1: Nucleic acid delivery vectors. The figure shows the viral vectors on the right side and the non-viral vectors on the left side represented by graphene-based, nanoparticles-based, lipid-based, polyplex-based and peptide-based vectors.*

Decreasing concerns of off-target effects[6]. Retroviruses have traditionally been used as they integrate into the host genome, yielding maintained expression of the transgene at adequate levels. Though, they are prone to induce insertional mutagenesis through integration in the host genome, driving to a significant risk of oncogenesis. Lentiviral is an alternative vector to conventional retroviral vectors. It shows lower risks of insertional mutagenesis and more efficient in transfecting both dividing and non-dividing cells[6].

Viral vectors suffer from limitation including side effects, e.g., allergic reactions, immunogenicity, host rejection, mutagenicity, and oncogenicity[7]. Furthermore, they lack scaling up production[8], and their costs are significantly high (in the range of $1 million per treatment)[9]. On the other hand, non-viral vectors are favored over viral vectors because of the lower risks of insertional mutagenesis, decreased regulatory requirements, reduced production costs, and lower endogenous immune activation[6].

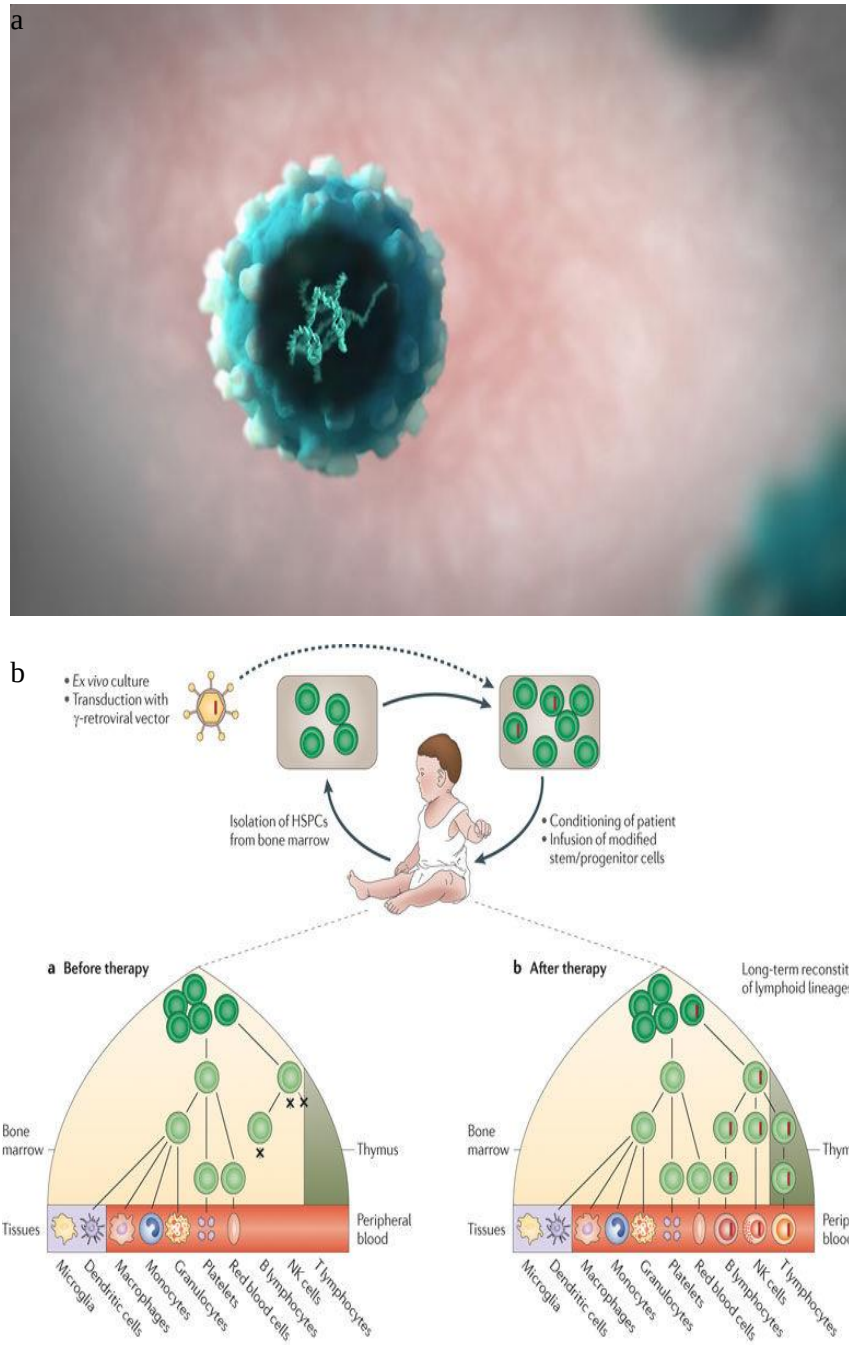


*Figure 2: a) Viral vector used as gene therapy for Strimvelis (Image and vector are made by Glaxo Smith Kline). b) Ex vivo gene therapy strategy. The images are re-printed with permission from Springer Nature Ref.9,10. Copyright belongs to Springer Nature.*

## 1.3. Non-viral vectors

The ON delivery using non-viral vectors includes the treatment of cells using chemical and physical methods. As an example, in 1990, Wolff *et al*. reported genes expression in mouse skeletal muscle upon injection of pure DNA plasmids[11]. However, naked ONs showed low transfection efficiency and were rapidly removed by the mononuclear phagocyte system and the reticular endothelial system (RES) system. Furthermore, the challenge of providing a constant formulation with nucleic acid stably mixed in the delivery media need to be formulated for consistent and reproducible ON delivery[12,13].

The ON delivery methods using non-viral vectors including cationic lipids, polymers, nanoparticles, and peptides are reported. These agents promote cellular targeting and nuclear localization. Non-viral vectors can reproducibly and reliably transfect the mammalian cell lines in vitro. Non-viral vectors are straightforward to scale up and show minimum host immune response (Figure 3). They are suitable for selected organs such as airway with mucosal tissue or lung as the target site, or for localized tissues, such as intratumoral targeting. However, non-viral vectors are in need for enhancing their efficacy and defining their final physicochemical features[14].

## 1.4. Peptides

Peptides, in common, are recognized to be a short chain of amino acids (~50 residues). Peptides can be chemically synthesized or obtained via extraction from a natural source[15]. A vast number of natural peptides are synthesized non-ribosomally using nonribosomal peptide synthetases. These natural peptides include the antibiotic daptomycin, the immunosuppressant cyclosporine A, and the anticancer drug bleomycin A2[16]. Peptides can be classified into three classes; 1) therapeutic peptides, which have high biological activity, 2) immunogenic peptides, that are used to promote an immune response toward an infectious or oncologic target, and 3) cell-penetrating peptides (CPPs) which are vectors for cellular delivery of nucleic acids, proteins, or small-molecule drugs[17].

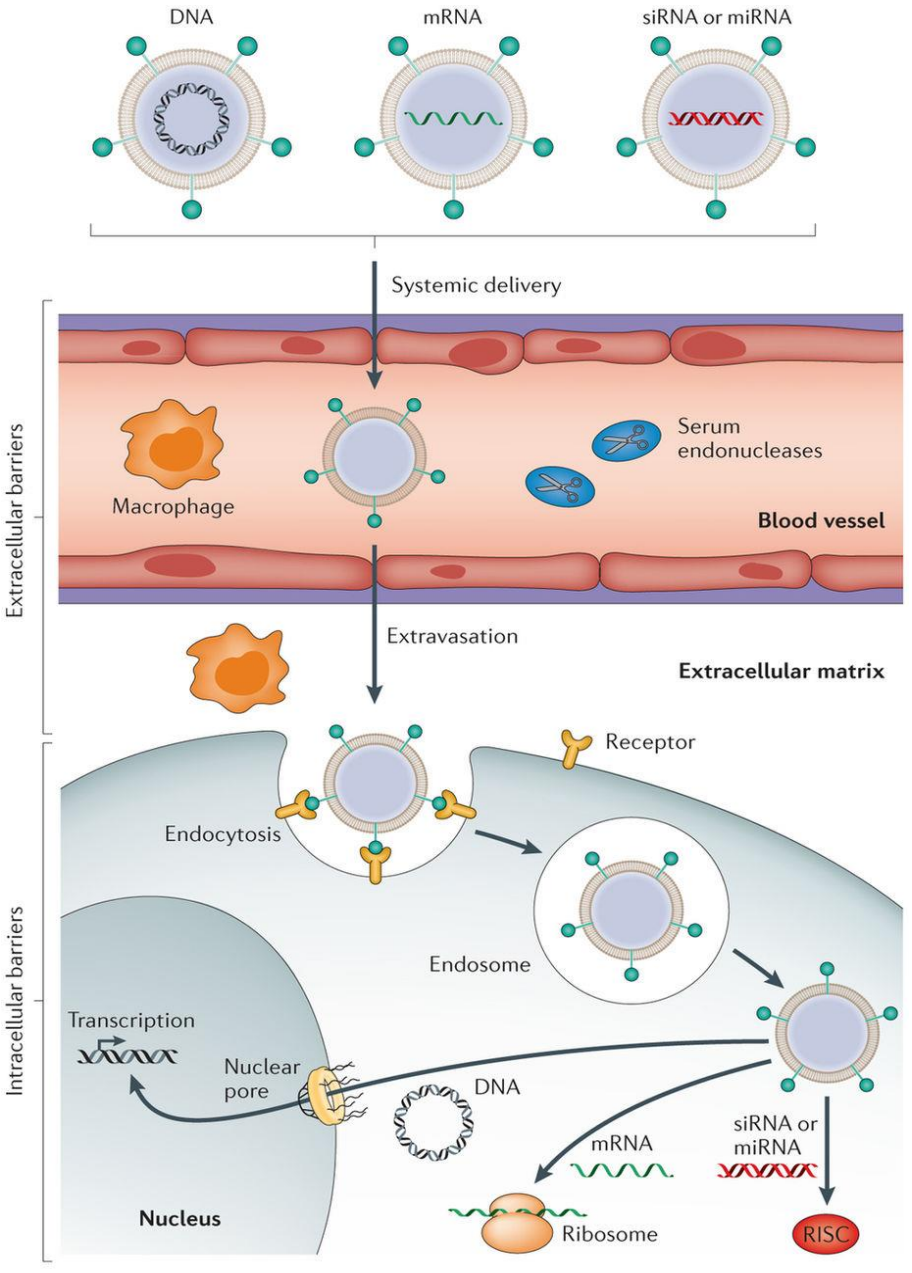


*Figure 3: Non-viral vectors are crossing barriers for gene therapy. The scheme shows non-viral vectors loaded with nucleic acid cargos and passing the blood vessels barriers then extracellular and cellular obstacles for doing its function. The image is adapted with permission from Springer Nature Ref.18. Copyright belongs to Springer Nature.*

## 1.5. Cell-penetrating peptides (CPPs)

CPPs, are short cationic peptides typically with < 50 amino acids, are efficient non-viral vectors[19,20]. CPPs have been applied used to deliver several types of agents including nucleic acids, proteins, small-molecule drugs, liposomes, lipid-based nanocarriers, polymeric nanoparticles, and dendrimers as well as biomacromolecules with significant cellular uptake efficiency and insignificant cytotoxicity[21–23]. Human immunodeficiency virus-1 (HIV-1) is the source of the trans-acting activator of transcription (TAT) protein that has cell membrane shuttling ability[21]; TAT is considered the prototype of CPP[22]. Since of TAT discovery, several thousands of different CPP have been identified from viral protein sequences as VP22 derived from Herpes simplex virus Type 1 (HSV-1) capsid protein[26].

On the other hand, other CPPs were from non-viral origin like penetratin originated from residues 43–58 of the third helix Drosophila Antennapedia homeobox protein[27,28]; and transportan originated from a neuropeptide galanin and wasp venom mastoparan sequences[29]. Furthermore, CPPs can be designed synthetically such as polyarginine[30], model amphipathic peptide (MAP)[31], and TP2[32]. PepFect3 (PF3) was designed based on TP10 sequence with stearic acid modification in N-terminal which is efficiently improved the cellular internalization. PF3 enabled non-covalent complexation strategy. PF3 condensed the splice correcting ONs (SCO) into nanoparticles that provided splice correction at low SCO doses[33]. PF3 is a capable transfection vector for plasmids delivery both *in-vitro* and *in-vivo*[34].

To improve the endosomal escape of PF6, endosomolytic modification of a lysine tree with pH titratable trifluoromethyl-quinoline derivatives was investigated. The endosomolytic moieties were coupled to the lysine side chain of PF3. PF6 showed high efficacy for siRNA transfection, shown in the effective knockdown of HPRT1 mRNA levels. PF6 improved over its parental peptide PF3 proved that PF6 had demonstrated pH-dependent endosomolytic features. Moreover, in the in-vivo treatment PF6/luc-siRNA complexes mediated knockdown in the liver without noticeable side effects and revealed the efficiency of PF6 for *in-vivo* treatment[35].

PF14 offered high stability against proteolytic activities. All lysines in the backbone were substituted with ornithines, and the sequence design was inspired by leucine zippers to improve ON binding affinity. PF14 revealed the remarkable efficacy of SCOs delivery for HeLa pLuc705 cells, mdx mouse myotubes, and Duchenne's muscular dystrophy in-vitro models[36]. Besides, PF14 formed a non-covalent delivery vector for siRNA that elicit an effective RNA-interference activity in several cell lines[37]. Moreover, PF14 revealed the feasibility to prepare PF14-SCO and PF14-siRNA transfection vectors into the solid formulation for therapeutic applications[36,37]. Furthermore, investigations demonstrated that PF14 is a standard CPP transfection vector for various ONs including short ONs and large pDNA. Effective ONs transfection and expression was achieved even in hard-to-transfect primary cells[38].

## 1.6. Amphipathic CPPs

Amphipathic CPPs contain both hydrophilic, and hydrophobic sequences of amino acids [39]. Thus, they can interact with both neutral and negatively charged lipid membranes[39]. Their sequences include non-polar amino acids, such as alanine, valine, leucine, and isoleucine, in addition to polar amino acids, including lysine[40]. The inclusion of hydrophobic moieties to the sequence of cationic amino acids enhances the transfection efficiency of cationic peptides by reducing their toxicities, by increasing their membrane perturbation efficiencies, and by improving their cellular uptake[41].

Amphipathic peptides can be categorized as primary or secondary amphipathic, based on the organization of amino acids in the peptide sequence. For instance, in primary amphipathic peptides, one terminus is mostly formed of hydrophobic amino acids, but the opposite end is enriched with hydrophilic amino acids. Additionally, in primary amphipathic CPPs, hydrophilic and hydrophobic domains are usually separated by a spacer sequence. Primary amphipathic CPPs cover peptides with protein origin (e.g., pVEC, originated from cadherin protein, and ARF (1–22), originated from p14ARF protein). Also, chimeric CPPs including a hydrophobic domain and the nuclear localization sequence (NLS) (e.g., MPG and Pep-1) have been reported. NLSs, lysine, arginine, or proline-rich short cationic CPPs can transport cargoes into the cell nucleus[22].

On the other hand, in secondary amphipathic CPPs, peptides include an even distribution of hydrophilic and hydrophobic amino acids on the peptide chain, and the separation of hydrophilic and hydrophobic chains is conformational in α-helical structure[42]. This CPPs which develop secondary amphipathic α-helix, a general structural motif in several peptides and proteins that interact with membranes, are involving penetratin[27], transportan[29], and MAP[31]. Distinctive from cationic CPPs, deletion and single point mutations without amphipathicity alteration may hinder cellular delivery of amphipathic CPPs[43,44]. The tryptophan modification for peptide structure was applied as a principle for additional changes, including the substitution of lysine with ornithine or arginine, also, phosphotyrosine modification to improve interactions with membrane phospholipids as in the case of the NickFect peptides[45].

## 1.7. Cell-penetrating peptides based on quantitative structure-activity relationship models (QSAR)

QSAR models can be used for the design of effective CPPs. Molecular dynamics and molecular docking modeling may provide us with valuable information for the illustration of the reasonable mechanisms of the interaction between CPPs and membranes, between a CPPs and cargo molecule[46]. Structure-activity relationships could be a helpful tool to make reasonable modifications of peptides. With the development of QSAR models, it could be used before attempting the synthesis of new peptides, and the synthetic work could be focused on promising candidates. Thus, researchers can save resources and reduce time-consumption for trial-and-error experiments.

## 1.8. Nanoparticles

Nanoparticles are described as particles or particulate dispersions with size < 200 nm[47]. Nanoparticles expand the opportunity for inventors, producers, and consumers of nearly all fields due to their unique properties at the molecular level[48–68]. Nanoparticles have a large specific surface area, possess high surface charge, and can be available with a

different geometry to mimic their biological counterparts. Nanoparticles have remarkable features which are usually absent in their bulk structure[69]. So nanoparticles are extensively investigated in the field of drug delivery. Several nanomaterials have been formed, including gold nanoparticles, cerium oxide nanoparticles, iron oxide nanoparticles, carbon-based nanomaterials, and polymeric nanoparticles. Nanoparticles have been applied for several applications including photonics, electronics, coating, cosmetics, and pharmaceuticals[70].

## 1.9. Magnetic nanoparticles (MNPs)

Iron oxide magnetic nanoparticles have drawn significant research interest for their application as drug delivery vectors enabling the usage of a magnetic field as external stimuli[56,71–79]. MNPs have been widely investigated in drug and gene delivery uses. Magnetic properties are essential in several biomedical purposes such as cell separation, magnetic resonance imaging, cell labelling, biosensing[80], as well as bio-separation and purification of nucleic acids[81], tissue repair, site-directed drug delivery and gene delivery[82,83]. MNPs were used for diagnosis and as a targeted therapy for cancer[84]. MNPs have unique physiochemical characteristics as high mechanical strength, large surface area to volume ratio, and high biocompatibility that enabled their high potential to enhance the efficiency of anticancer drugs and overcome the multidrug resistance. FDA approved MNPs as magnetic resonance imaging (MRI) contrast agents, and for clinical trials of other biomedical applications[85,86]. MNPs moreover act as effective localized heat sources, which has been used for hyperthermia induction as anticancer hyperthermia therapy[87].

## 1.10. Clinical trials using MNPs for hyperthermia therapy

MNPs have been investigated in several clinical trials, mainly in recurrent tumors. The workability, tolerance and the temperatures obtained by MNPs were estimated in 22 heavily pre-treated recurrences in patients with different histopathologies (ovarian cancer, cancer cervix, rectal cancer, prostate cancer and sarcoma)[88]. MNPs were injected either intraoperatively under direct visual control, under CT fluoroscopy or transrectal ultrasound (TRUS). The procedure was appropriately tolerated and was done with the magnetic field applicator applying magnetic field strengths altering in a range from 3 to 10 $kA \cdot m^{-1}$ depending on the targeted tissues: pelvis, neck, thorax, and the head. The magnetic field activation of the MNPs achieved the temperature of 40 °C with an objective coverage of 86% of the target tissues. Majority of the patients encountered subjective feelings of heat stress; however, this did not limit treatment, and the subacute toxicities were moderate at one year[88].

In the context of recurrent prostate cancer, Johannsen *et al*. described the use of MNPs suspensions in ten patients entered on phase I clinical trial[89]. High temperatures > 55 °C could be accomplished within the prostate, and the MNPs could be identified even after a year in the prostate, showing that a single treatment was enough[89]. No systemic toxicity was recognized through the median follow-up of 17.5 months (3–24), and the quality of life was only briefly impaired. A reduction in prostate-specific antigen was remarked in eight of the ten patients[89].

The common considered data for the clinical treatment of nanoparticles appears from the application of magnetic fluid hyperthermia for treatment of recurrent glioblastomas. MNPs with 12 nm size coated with aminosilane was injected into recurrent glioblastomas before twice weekly hyperthermia therapy using a 100 kHz alternating magnetic field. The median survival duration of 13.4 months recorded in 59 patients is considerably longer (10.6–16.2 months) than the average six months median survival spans regarded in this patients[90]. The treatment was pretty well tolerated, and post-mortem investigations remarked that nanoparticles were localized to areas of tumor necrosis and confined within macrophages[91].

## 1.11. MNPs for nucleic acid delivery

MNPs mediated gene transfection, and targeting was reported. Magnetic biomimetic contrast agents were formulated to have dual functions: being active for nucleic acid delivery and magnetic detection. These nanoparticles were formed of functionalized MNPs cores. The shell can be composed of a silica layer, an inert gold layer, or a layer of inert metal seeds. The outer corona of these nanoparticles is usually formed of gold–silver nanoshell and a targeting ligand connected to the inactive metallic nanoshell. These nanoparticles can be used for magnetic resonance imaging, ablating atherosclerotic plaque or treating primary or metastatic cancers. Non-viral nanoparticles delivery vector was generated for siRNA transfection. The siRNA delivery vehicle was composed of an MNPs core and a shell of alkylated polyethyleneimine. The knockdown efficacy of the siRNA-loaded vectors was evaluated in 4T1 cells and with xenograft model. Significant knockdown of luciferase was achieved, and distinctive from high-molecular-weight analogs, the coated particles showed biocompatibility[92].

MNPs could be applied to improve gene delivery of viral vectors[93] and non-viral vectors[94]. In before-mentioned systems, the ONs are associated with MNPs, and the transfection of the targeted cells was achieved by the use of high-field/high-gradient magnets[95]. The delivery efficacy of this technique is similar to commercially available ONs delivery vectors such as Lipofectamine[95]. The enhancement of the overall delivery levels was accomplished by applying an oscillating magnet array system with data indicating an increase of the in vitro delivery levels in human airway epithelial cells compared to Lipofectamine and static field techniques[95]. Fouriki *et al*. studied the influences of a nonviral oscillating magnet array system in improving ONs delivery effectiveness of primary human mesenchymal stem cells (hMSCs)[96]. Green fluorescent protein (GFP) encoding plasmids were conjugated to MNPs and used to transfect hMSCs in vitro. Magnetic fields produced by magnets positioned under the cell culture plates offers a simple method for direct target the MNPs-DNA to the cells. The oscillation of the magnetic arrays raised higher efficient endocytosis through mechanical stimulation. Thus, delivery efficacies, as well as cell viability, were enhanced.

Furthermore, the expression of hMSC-specific cell surface markers was unchanged from normal levels. This technique improved the delivery of plasmids to MG-63 osteoblasts, adult cardiomyocytes, and NIH3T3 mouse embryonic fibroblasts cell lines[97]. In another report, Kijewska *et al*. modified MNPs by polypyrrole microvessels[98], and the nanocomposite showed superparamagnetism. mRNA cap analogs with anti-cancer activity were encapsulated in the core of the microvessels, and an external magnetic field was applied to triggered the mRNA cap diffusion throughout vessel walls. The cap structure was conserved through the process of encapsulation and release[98].

The small size of superparamagnetic iron oxide nanoparticles (SPIONs, size < 10 nm) enhance the cells internalization and thus, promote uptake of these nanoparticles by cells. Wang *et al*. proposed that the conjugation of TAT peptide to SPIONs could increase the cellular uptake of these nanoparticles[99]. Flow cytometry measurements showed that TAT-decorated SPIONs had enhanced cellular delivery, and their improved accumulation compared to the unmodified SPIONs is owing to the cationic charge of the TAT CPP and its total cationic zeta potential. In another investigation, conjugation of the ϒ-amino-proline-derived CPP with SPIONs improved the delivery of these nanoparticles into the COS-1 and HeLa cell lines over the analog TAT–SPION. Hence, this CPP was used to compose effective bimodal imaging materials[100]. The stability of these CPPs towards protease degradation is provided by the ϒ-peptide skeleton. They showed low cytotoxicity. Harris *et al*. reported dual functions using MNPs with R6 and MMP-cleavable PEG[101].

## 1.12. Graphene-based Nanomaterials

Graphene is a separated monolayer of graphite[102]. Graphene-based nanomaterials have unique chemical properties due to their structure that consists of a single flat layer of carbon atoms packed into a hexagonal arrangement with $sp^2$ hybridization as 2D honeycomb lattice. This lattice is a fundamental building block for all other graphitic materials. Graphene structure reveals unique physical-chemical properties including large surface area, electronic flexibility[103–105], and optical, thermal, mechanical properties[106]. These valuable properties permit its applications in different fields as flexible electronics, hydrogen storage[107], biosensing[108], DNA sequencing[109] and others[110–118]. Graphite (stacked-up graphene monolayers), single-walled carbon nanotubes (SWCNTs, rolled-up graphene monolayers), and fullerenes (wrapped-up graphene) were reported for gene delivery[119]. Graphene oxide (GO) and reduced graphene oxide (rGO) are developed after oxidation and oxidation/reduction processes of graphite, respectively[120]. GO has the potential for biological and biochemical applicability since it is rich by oxygen-containing functional groups and shows high dispersion in water and other polar solvents[121].

In 2008, Dai *et al*. described the synthesis of nanoscale GO as a drug delivery vector[121]. They reported that the polyethylene glycol (PEG)-modified GO could be used to load doxorubicin the anti-cancer drug by hydrophobic π stacking and induce apoptosis of cancer cells in vitro. Following that, graphene has been considered as an attractive nanocarrier for drug delivery due to various reasons[122,123]. It has a two-dimensional single layer structure, which could give a larger surface area. It has been published that the packing mass of drugs could be 200% of the graphene-based drug vector[124]. Secondly, graphene-based derivatives have a leading chemical and mechanical stability[125], enabling graphene-based nanomaterials suitability for various delivery conditions.
Furthermore, the surface modification of graphene and its derivatives via the formation of covalent or non-covalent bonds is straightforward process[126]. Thus, it can be used for nanohybrids materials. Graphene-based nanomaterials have powerful optical adsorption in the near-infrared range, proposing them as leading agents for photothermal and photodynamic therapy[127,128].

## 1.13. Graphene mediated nucleic acid and protein delivery

Graphene-based nanomaterials are suitable vectors for nucleic acid delivery due to their high loading capacity and enhanced ONs transfection efficacy. Graphene-based nanomaterials were modified by polymers, such as polyamidoamine (PAMAM)[98], chitosan[129], and polyethyleneimine (PEI)[130]. Zhang *et al*. applied PEI-conjugated GO for cell transfection for siRNA and doxorubicin (DOX)[131], presenting a synergistic influence that led to significantly enhanced biological efficiency. Liu *et al*. investigated the potential of PEI-functionalized GO for ONs delivery using various molecular weights of PEI[132]. They reported that the materials have low cytotoxicity and are potent for ONs transfection nanocarrier with high delivery efficacy. GO functionalized lactosylated chitosan oligosaccharide (GO-LCO) was synthesized for the targeted transfection of ONs to human hepatic carcinoma cells (QGY-7703)[133]. The loading capacity of FAM-DNA was high, and it was delivered to QGY-7703 within 0.5 h. Besides, no apparent toxicity was noted even at significantly high concentrations. Hu *et al*. synthesized GO modified folate-conjugated trimethyl chitosan (GO-FTMC) via electrostatic self-assembly to investigate the targeted transfection of plasmid DNA (pDNA)[129]. The presence of FTMC could delay the movement of pDNA and promote pDNA condensation. Liu *et al*. prepared graphene-oleate-PAMAM dendrimer hybrids through oleic acid adsorption accompanied by covalent linkage of PAMAM dendrimers as ONs transfection vectors[98].

Graphene-oleate-PAMAM showed good dispersion in aqueous solutions and high biocompatibility for HeLa cells but exposed cytotoxicity to MG-63 cells at concentrations >20 mg/ml. Graphene-oleate-PAMAM loaded pEGFP-N1 (25%) showed a GFP gene delivery efficacy of 18.3% using HeLa cells. GO modified with PAMAM dendrimer-grafted gadolinium[134], and mPEGylated GO conjugated with poly(2-dimethylaminoethyl methacrylate)(PDMAEMA) nanohybrids[135] were prepared for RNA transfection to enhanced the cellular delivery efficacy and the biocompatibility. Teimouri *et al*. developed three GO-based vectors for ONs transfection based on the conjugation of GO with cationic polymers of PEI, polypropylenimine (PPI), and PAMAM to compare their cytotoxicity and delivery efficacy[130]. GFP was used to estimate the cellular delivery efficacy, and the data revealed

that PEI-GO conjugate was nine-fold higher efficient in the EGFP-transfected cells. Choi *et al*. prepared GO-PEI complexes to load mRNA for clinical applications efficiently[136]. They reported that human induced pluripotent stem cells (iPSCs) could be produced from adult adipose tissue-derived fibroblasts without the need for repeated daily transfection[136].

Furthermore, proteins can be transfected using graphene-based vectors. Zhang *et al*. described the co-delivery of ribonuclease A and protein kinase A to the cell cytoplasm avoiding enzymatic hydrolysis and loss of biological activity, by using GO-PEG for loading proteins through noncovalent interactions[137]. Hong *et al*. used multilayer GO-poly (β-amino ester) as a delivery vector for ovalbumin, a protein antigen[138]. Data showed that the multilayer films prevented the initial release of ovalbumin and could be accurately controlled to promote ovalbumin release by the use of electrochemical potentials. Additional models involve loading GO-coated Ti substrate with bone morphogenic protein-2 (BMP-2) to improve the differentiation of human mesenchymal stem cells (MSCs), which further revealed robust new bone generation with this Ti-GO-BMP2 implant[139]. Moreover, Geest *et al*. described the intracellular protein vaccine transfection of GO-adsorbed proteins that could be internalized efficiently by dendritic cells and improved antigen cross-presentation to CD8 T cells[140].

## 1.14. Autophagy

Autophagy is a catabolic pathway that controls nutrient regeneration through degradation of nonfunctional proteins and organelles via lysosomal-mediated degradation[141]. Autophagy is commonly admitted as cytoprotective pathway protecting from neurodegenerative diseases, a diversity of clinical interruptions are leading to enhance autophagy as a therapeutic strategy. Autophagy happens constitutively at a basal rate supporting normal cellular conditions to keep homeostasis for metabolic regulation and intracellular recycling. Autophagy is promoted through several pathological and physiological states as starvation. The cells react to these situations by transforming these signals into various catabolic and anabolic responses. The cells catabolize the damaged cellular elements for producing substrates for supporting adenosine triphosphate (ATP) generation through times of nutrient need[142].

Autophagy pathway includes the generation of unique structures that isolate the target materials (cargo), engulfs and delivers them into the autolysosomes for degradation[143]. Based on the method of delivery of cargo into the autolysosome, three kinds of autophagy have been distinguished: microautophagy, macroautophagy, and chaperone-mediated autophagy. Microautophagy is the cellular degradation pathway where the lysosomal membrane elongates to invaginate the target contents. Electron microscopy images show a linear relation of the number of microautophagic structures with the targeted protein turnover[144]. Macroautophagy is the second kind of autophagy which includes the generation of specialized structures called autophagosomes to entrap the targeted contents[145]. After that, the autophagosome fuses with a lysosome for degradation. The pathway is constituted of a series of events concerning the formation of the autophagosome, its fusion with the lysosome and finally the degradation[146]. Macroautophagy is the primary pathway done by the cells to degrade the defected cellular organelles and other similar debris. The third kind of autophagy is the chaperone-mediated autophagy (CMA). This pathway demands a motif peptide sequence with pattern homologous to KFERQ sequence in proteins for degradation. The proteins holding this motif sequence are identified by HSC70, a chaperone protein that carries them to the lysosomal membrane. The proteins are then brought into the lysosome by a membrane receptor called LAMP-2A and are degraded in the lysosomal lumen. This pathway is specific as the degradation is restricted to the proteins

that have the motif sequence. CMA regulates the proteasomal degradation of proteins and controls their cellular levels[147].

Autophagy role in cancer development is still unclear and under investigation. Although, cancer is the disease where notable current investigations by trying to manipulate autophagy for therapeutic development is studying, and handfuls of clinical trials are using autophagy interference with chloroquine or hydroxychloroquine in association with various medications for the therapy of multiple neoplasms[148]. Autophagy helps cells to sustain intracellular homeostasis and respond to stress by degrading organelles, proteins, and several cellular elements through the lysosomal degradation pathway. Abnormalities in autophagy and acquired mutations in autophagy-related genes, known as ATG genes, which regulate autophagy have been connected with human diseases, like neurological diseases, infectious disease, metabolic disorders, autoimmune diseases, and cancer. These connections reveal that therapeutics to induce or inhibit autophagy can be advantageous to treat or inhibit disease[149].

## 1.15. Manipulating Autophagy for Therapy

Autophagy is controlled transcriptionally by MITF and FOXO groups of transcription factors[150], as well as ATF and CREB[151], and is further regulated through post-translational modifications enabling its pharmacological manipulation both positively and negatively[152–154]. For instance, the mammalian target of rapamycin (mTOR) complex mTORC1 inhibits autophagy. Accordingly, mTOR inhibitors are commonly used to stimulate autophagy. mTORC2 has been connected to autophagy, despite this may be specific for CMA[155]. Independent of mTOR regulated autophagy, the naturally occurring disaccharide, trehalose, that acts independent of mTOR[156], induces autophagy to protect from several liver diseases by altering glucose transporters[157].
Macroautophagy is controlled by nutrient availability through regulation by mTORC1, that next situation of nutrient availability can inhibit the induction of Ulk1/2 complexes. ULK complexes stimulate Beclin-1 complex[148]. Further medications inhibit autophagy via inhibitors of the protein kinases, ULK1, ULK2 and the class III phosphoinositide-3-kinase (VPS34)[158]. VPS34 is a protein member of the BCL-2 interacting

moesin-like coiled-coil protein 1, (Beclin-1) signalling complex. Beclin-1 includes a BH3 domain, allowing it to interact with other BH3 containing proteins, covering B-cell CLL/lymphoma 2 (BCL-2)[159].

The downstream functions of the Beclin-1 complex can modify autophagy influence, based on the molecules forming the complex beside it[160]. Further components of the complex include ultraviolet irradiation resistant-associated gene (UVRAG), SH3GLB2 (BIF-1), and activating molecule in Beclin-1 regulated autophagy 1 (AMBRA1). Part of these interactions can be pharmacologically manipulated. BH3 mimetics as Venetoclax, which was designed to stimulate apoptosis by interrupting BCL-2 synergies at the mitochondria, moreover, prevent interactions between Beclin-1 and BCL-2 to induce autophagy[161]. Though this pathway has been investigated, and it has been proposed that BH3 mimetics may only promote autophagy by auxiliary mechanisms that happen following they have hit their target[162].

A modified CPP, Tat-Beclin1, prevented interaction in the Beclin-1 complex to begin autophagy[163]. Alongside the different medications that can manipulate autophagy[164], non-pharmacological strategies like exercises and caloric restriction further influence autophagy. For example, physical training targets the Beclin-1 signalling complex to begin autophagy that can protect mice from diabetes[165].

The ubiquitin-like protein ATG12 reveals an interaction with ATG5 in a pathway dependant on the E1-like enzyme, ATG7. A similar lipid conjugation system (using ATG7) connects phosphatidylethanolamine (PE) to the Microtubule-Associated Protein 1 Light Chain 3 (MAP1LC3), further GABA type A receptor-associated protein (GABARAP) groups of proteins. LC3-PE complexation is following cleavage and processing of LC3 by the protease, ATG4B, that can be inhibited pharmacologically[166]. The final step is a fusion of the autophagosome with the lysosome, mediated by the SNARE protein STX17[167]. The action mentioned before can be blocked with lysosomal inhibitors like Bafilomycin A1, chloroquine (CQ) or hydroxychloroquine (HCQ). When fusion is complete; the lysosomal hydrolases degrade the cargos of the autophagosomes giving nutrients, amino acids, and lipids that are provided to fuel protein synthesis and other macromolecular production and metabolism[148].

# 2. Aims

This thesis aims to develop novel drug delivery vectors with high efficiency including targeting ability. Furthermore, it discusses the cellular uptake mechanism.

## 2.1. Paper I

Peptide-based nonviral delivery vectors are a promising class for delivering gene therapeutic agents. In silico design is one of the strategies for improving the efficiency of the peptide-based gene therapy vectors. The method can be used for the design of new peptides based on the structure-activity knowledge of former peptides. For designing CPP transfection vectors based on an FQSAR relating earlier described peptide model amphipathic peptides. Various QSAR models were generated to refine and enhance the predictability of the biological effect for the predicted peptides. The current FQSAR models aimed to produce new sequences to study the function of the sequence of the peptides on the uptake potency. Then, the predicted peptides were synthesized and examined for biological activity.

## 2.2. Paper II

Applications of nanoparticles are investigated as co-nonviral vectors with CPPs. Nanoparticles offer new possibilities for the gene or drug delivery. Magnetic nanoparticles in assembling drug or gene delivery vectors are promising due to their efficacy for the drug delivery, the easy modification of its surface and being biocompatible. Magnetic nanoparticles offer selective targeting for drug delivery vectors based on

its magnetic properties enabling magnetic targeting for the new vectors. Magnetic nanoparticles can protect the gene therapeutic agents assembled in the new vectors against nuclease degradation and enhance their stability. The cationic surfaces of magnetic nanoparticles can assist the assembly of the nucleic acid cargos of the gene delivery vectors as the nucleic acids have anionic phosphorothioate groups enabling electrostatic interactions with the cationic magnetic nanoparticles.

## 2.3. Paper III

Paper III aimed to have higher biological efficacy, by using Graphene oxide (GO) as a building block for the nucleic acid delivery vectors. GO offers a high aspect ratio and surface area which is approximately ten fold of other nanomaterials with high biocompatibility[168]. Graphene oxide enables the design of smart vectors for drug delivery and tissue-specific targeting controlled drug delivery vectors, providing bimodal photothermal and photodynamic therapy for tumors. The conjugation of GO nanosheets with biomolecules including CPP and nucleic acid cargos is simple and can advance new vectors with multifunctional applications.

## 2.4. Paper IV

The uptake process of CPP is kinetic, so the RNA expression pattern reflects the sub-cellular responses triggered by transfection. Here, we aimed at investigating the gene expression profiles of transfected HeLa cells by performing RNA sequencing analysis and associating it with cellular pathways that might be controlling the transfection process. Additionally, we have confirmed the regulation of identified genes by transfection studies conducted in the presence and absence of small molecule ligands these particular gene products.

# 3. Methodological considerations

In this thesis, several analytical methods were used for the synthesis, characterization, and application of cell-penetrating peptides. A brief description of these techniques is presented in this chapter.

## 3.1 Cell-penetrating peptide design

A standard peptide model is usually required to investigate the efficiency of CPPs. We selected PF14 as an active model peptide to be used in this thesis as a control for the novel designed peptides, hybrid oligonucleotide delivery vectors, and in the uptake pathway investigation. Also, data of former PepFect CPPs were used to be fragmented in biological-structural-based aspects to feed a model for the designing of the new peptides.

## 3.2. Structure-activity relationships

Structure-activity relationships correlate results of various peptides, such as the biological response to the design of the peptides. Quantitative structure-activity relationship (QSAR) models can be used for theoretical prediction of peptides (virtual screening). Retrieved QSAR models may shed light on activity, mechanisms of action, a possible selectivity of peptides, etc.[169]. Therefore, in the paper I, a quantitative structure-activity model was designed to correlate the physiochemical properties of the studied peptides to its biological activity (in this case the measured luminescence after peptide-mediated delivery of a luciferase-encoding plasmid). QSAR analyze various descriptions of predictors and a computer-based relationship of related element parameters.

The purpose of QSAR modeling is to identify geometrical correlations between the predictors and the activity of a compound. Modelling in QSAR gives predictions that can be validated compared to the dataset itself or by using an external dataset. The basic theory of all QSAR models is that related molecules maintain relevant characteristics[170].

In the paper I, the QSAR model was designed based on 200 molecular characteristics of the parent peptides to be descriptors per peptide as independent variables, determined with Assisted Model Building with Energy Refinement (AMBER) molecular mechanics (Hyperchem, hyper.com). In the QSAR model, all peptides were assumed to have α-helical structures. Initial models were designed using the program FQSAR Model, and the models having best matching descriptors for the experimental biological result were chosen.

## 3.3. Solid-phase peptide synthesis

The newly peptides were designed based on the developed QSAR model solid-phase peptide synthesis (SPPS). SPPS is a standard technique for the synthesis of peptides for both research and therapeutic prospects. Purification is usually used after coupling of every amino acid. The purification takes places by chromatography and extraction using silica gel columns. The process is a time-consuming process. In 1963, Merrifield developed the SPPS approach for synthesizing peptides[171]. The peptide is attached physicochemically through its C-terminus to a solid phase, which allows for filtration to be used to replace consumed reagents with fresh reagents for the next step of the reaction. In this thesis, the peptide was synthesized using a stepwise sequence of amino acids addition through coupling followed by de-protection of every amino acid. Addition occurs through amide bond formation between the carboxylic acid of the new amino acid to a free amine on the attached peptide chain growing on the resin support. In the Fmoc scheme, the peptide is connected to the solid support by an acid liable linker. As a way to make the reaction specific, amino acids with a protection group hiding their α-amine are used for the coupling addition; the protection group is 9-fluorenylmethyloxycarbonyl (Fmoc). This

group is efficiently separated from the amino acid (or deprotected) using a base like piperidine or piperazine. The amino acid side-chains are protected with acid labile groups. After attachment of each amino acid, the Fmoc group is removed before the next amino acid is coupled. When the full sequence of the peptide is synthesized, the resin solid support and protection groups of the side chains are cleaved by using acid, generating an unprotected peptide.

All investigated peptides were synthesized using one of two automated peptide synthesis machines (Syro II, Multisyntech GmBH or Alstra+, Biotage AB, Uppsala, Sweden). The peptide was modified using stearic acid. All peptides were synthesized using an H-Rink-Amide-ChemMatrix resin (PCAS Biomatrix, St-Jean-sur-Richelieu (province of Quebec), Canada), this kind of resin gives peptides with amidated C-termini. The peptides are cleaved from the resin, by using 95% trifluoroacetic acid (TFA), 2.5% $H_2O$ and 2.5% triisopropylsilane (TIS), and then cleaved peptides were precipitated in ether followed by lyophilization. Reversed-phase high-performance liquid chromatography (HPLC) was used in Crude peptides purification using semi-preparative column. Pure peptides masses were measured using matrix-assisted laser desorption/ionization-time of flight mass spectrometry (MALDI-TOF-MS). The purified peptides with exact masses were lyophilized over then dissolved in ultrapure water (Milli-Q, Merck Millipore) before use.

## 3.4. Characterization of the peptide-based vectors

### 3.4.1. Dynamic light scattering

The particles size is an important key parameter that influences their characteristics and safety in biological systems. Dynamic light scattering (DLS), can be called as photon correlation spectroscopy (PCS) or quasi-elastic light scattering, is used to measure the particle size distribution in solution. DLS is based on fluctuations generated by the Brownian diffusion of spherical particles, where the Brownian motion of the particles is associated to a comparable hydrodynamic diameter.

The measuring instrument focuses a beam of laser light into the nanoparticle solution, and a photon detector estimates the intensity of the Doppler shift of the incident radiation, this intensity is time-dependent on the fluctuations. The sizes of peptides complexed with ONs as particles are calculated by using the Stokes-Einstein equation which correlates the timescale of particle diffusion to the comparable sphere hydrodynamic diameter of the particle. This relation is based on both the temperature of the samples and the viscosity of the solutions[172].

### 3.4.2. Zeta (ζ)-potential

The superficial charge (zeta potential, ζ) of nanoparticles including CPPs affects their efficiency. ζ-potential is the difference in potential between the stationary layers of fluid associated with a dispersed particle corresponding to that of the dispersion medium. Z-potential measurement is based on the electrophoretic velocity that is proportional to the electrophoretic mobility. Our measurements take placed using Zetasizer Nano ZS (Malvern Instruments, Malvert, UK).

### 3.4.3. Electron microscopy

The imaging of nanoparticles using electron microscopy (EM) has been advanced materials and biological applications[173]. Our understanding of nanoparticles and peptides structures is based on various EM contributions. As in many other fields in materials chemistry and biology, EM has made exceptional contributions to the understanding of the drug delivery vectors structure and its relationship with biological function. So, we used transmission electron microscopy (TEM) and scanning electron microscopy (SEM) in the characterization of our new drug delivery vectors in papers II, III, and IV.

### 3.4.4. Confocal microscopy

The development of confocal microscopes was inspired considerably by the need to image biological events as they occur in cells. Marvin Minsky built a confocal microscope in 1955 with the aim of imaging neural networks in unstained specimens of living brains. All of the standard confocal imaging systems apply the principle of confocal imaging that Minsky patented in 1957[174].
Live cell microscopy of fluorescently labelled ONs offers visualization of our peptide vectors delivery process. Accordingly, in this thesis uptake investigations were done in the proper physiological context, that is, on living cells in the papers II and III and under relevant stimuli from small molecule ligands regulating protein function to investigate its role in the uptake process in paper IV. Confocal microscopy provided a sensitive and fast tool to document individual molecular activities reliably.

## 3.5. Cell culture and treatment

HEK-293 (human embryonic kidney), HeLa (Human ovarian cancer), and HeLa pLuc705 cell lines were used as in vitro models. HeLa pLuc705 cells are a gift from Prof. Ryszard Kole (University of North Carolina, Chapel Hill, NC, USA). HeLa pLuc705 cell line is stably transfected with a luciferase-encoding gene interrupted by a mutated β-globin intron 2. All cell lines used in this thesis are immortalized lines, which are straightforward to sustain and grow active in the lab. HeLa is the eldest stable human cell culture and is the commonly used cell line in the world[175]. The HeLa pLuc 705 cell line was used in luciferase-based splice-correction assays[176]. HEK cells are a different broadly used model system; the cells were generated from a kidney cell culture exposed to adenovirus type 5 DNA[177], although the exact cellular origin is unknown and it could be neuronal. Cells were grown in incubator maintaining 5% $CO_2$, 37°C, in Dulbecco's modified Eagle's medium with glutamate supplemented with 10% fetal bovine serum, 0.1 mM non-essential amino acids, 200 U/ml penicillin, and 200 μg/ml streptomycin (Invitrogen, Stockholm, Sweden).

## 3.6. Luciferase assay

Reporter assays are widely applied for the screening of ONs delivery in-vitro and in-vivo[178]. So, for measuring the nucleic acid delivery efficiency by the peptides investigated in this thesis luciferase assay was used. Luciferase enzyme is a common reporter gene that catalyzes bioluminescence reactions and is used most commonly because it is sensitive and has linear response range that is superior to those of regular reporters including β-galactosidase, β-glucuronidase, chloramphenicol acetyltransferase and fluorescent proteins[179].
Bioluminescence is a straightforward reaction that is triggered by the addition of luciferin solution to the lysed cells expressing luciferase enzyme. Luciferase is a suitable reporter enzyme for the quantitative measurement of gene expression indicating the quantity of ON delivery. So, transfecting a luciferase encoding plasmid to a cell that does not ordinarily express the enzyme produces a measurable increase in light yield that is linearly related to the quantity of luciferase expressed in the cells. Also, transfection of siRNA of luciferase to a cell that now expresses luciferase will be presented in a decrease of enzyme and consequently a reduction in light generation.

## 3.7. Plasmid transfection assay

In the papers I, II and III the rLuc (renilla Luc) luciferase plasmid-based uptake assay was used for estimating the new peptide-based vectors efficacy in the delivery of plasmid DNA. A firefly luciferase expressing plasmids were transfected into the cells by non-covalent complex formation with peptides in charge ratios concentrations based on calculations of the positive charges of the peptides and the negative charges of the plasmid. Following addition of the complexes, the cells were incubated for 24 h; then the cells were lysed, followed by the addition of the luciferin substrate and luminescence measurements. The luciferin substrate was a commercial luciferase assay kits containing coenzyme A with luciferin together for enhanced light intensity and stability. In the papers, II and III, hybrid peptide and nanoparticles-based vectors were formed by the non-covalent addition of the nanoparticles to the plasmids before addition of the peptides.

## 3.8. Splice correction assay

In all papers, the splice correction test, was developed by Kang *et al*., implements a refined quantitative assessment of the cellular delivery potency of SCOs. The test is based on HeLa cells that have been stably transfected with luciferase-expressing plasmid pLuc 705, in this case, the plasmid is containing a luciferase-encoding gene disrupted by a mutated intron from a β-thalassemic globin gene. The intronic mutations result in a splice site that is expressed in non-functional luciferase. Blocking the mutation site using antisense ON restore the splice correction machinery to generate functional luciferase enzyme. In papers II and III, the splice correcting hybrid vectors were formed by the addition of the nanoparticles to the SCO before complexation with the peptides.

## 3.9. RNA sequencing

RNA sequencing was used to investigate the influence of the cell penetrating peptide as a delivery vector on the RNA expression levels. Global gene expression investigations with total RNA sequencing offer a high-throughput method for the identification of genes and gene networks associated with the peptide transfection. Progress in this high-throughput technology over the past two decades has directed to innovative insights into the uptake mechanisms of drugs and their delivery vectors. Till recently, the microarray has expressed the most important method to study gene expression regulations[180,181]. Though the microarray relies on an indirect quantification by hybridization, resulting in various weaknesses including high background as result of cross-hybridization[182], and the need for prior knowledge of sequences to be investigated. RNA-Seq has achieved growing prevalence and replaced microarrays as the principal high-throughput option for quantifying the whole transcriptome[183]. RNA-Seq is based on next-generation sequencing that directly resolves the cDNA sequence. It efficiently overcomes the limitations of microarray: a previous sequence knowledge is not needed; various layers including exon, gene-level and isoform quantification can be measured; and broad dynamic range can be investigated[184]. RNA-Seq technology has presented an ideal method to examine the transcriptomic regulations shedding light on uptake pathways of our peptide transfection model in paper IV.

# 4. Results

## 4.1. Paper I

In the first paper, we used two sets of newly designed peptides based on the two independent fragmentation schemes and applying the corresponding structure-activity relationship. Every fragment library was used to develop hundreds of new peptides in a combinatorial way, and the relevant FQSAR models were used to predict the LogBE. The new peptides with a LogBE value higher than five but below seven were investigated. For each fragmentation scheme, the best eight peptides regarding the predicted LogBE were analyzed for more selection. Thus, the number of predicted peptides was decreased to 16 peptides. Following the fundamental analysis, the work focused on the best five peptides for more chemical synthesis and biological tests. For the biological activity measurement, the newly designed and synthesized peptides were used for pGL3 plasmid transfection, and the luciferase assay was used to measure the luminescence indicating the efficacy of the delivery of each new peptide compared to control peptide PepFect 220. Statistical analysis by two-way ANOVA revealed that PepFect 220 and PepFect 221 were more capable of delivering the plasmids inside the cells than PepFect 21. PepFect 224 peptide was equivalent to PepFect 21.

## 4.2. Paper II

In paper II, CPP assembly MNPs and nucleic acid cargos were investigated. CPPs PF220, PF221, PF222, PF223, PF224, and PF14 were tested in complexation with a plasmid (pGL3), SCO and siRNA with and without MNPs were examined (Scheme 1). The morphological study of PF14 was done using SEM. SEM revealed that PF14 particles have sizes in the range of 100–500 nm. The morphological analysis of

the newly assembled vectors with and without the MNPs was investigated using SEM. SEM images were used for characterization of the morphologies of CPP/ON complexes with and without the MNPs.

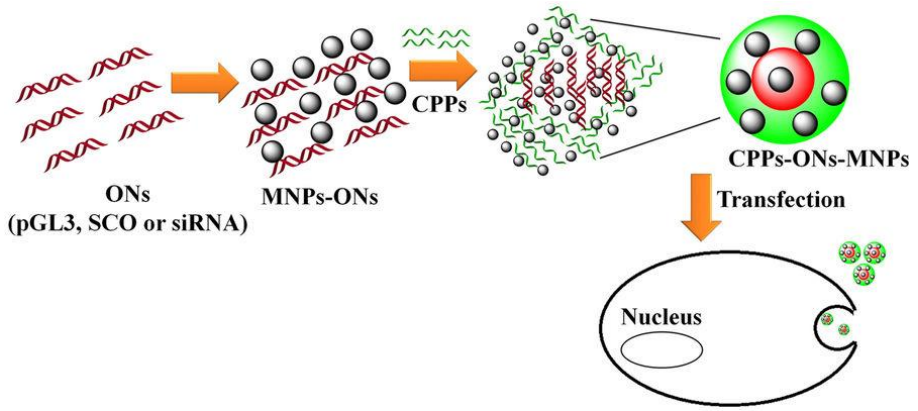


*Scheme 1: Formulation of the nucleic acid delivery vector by assembling with MNPs first then adding CPPs to transfect the cells. The image is adapted with permission from Ref.185 (Paper II).*

The characterization of PF14/pGL3, PF14/SCO, and PF14/siRNA showed aggregation of the subunits, and the MNPs demonstrated distribution in the complexes of CPPs/ONs. SEM showed the characteristic well-defined morphology of PF221/pGL3/MNPs, PF220/SCO/MNPs, and PF14/siRNA/MNPs in compared to the other CPPs/ONs/MNPs. PF221/pGL3/MNPs is formed from subunits of the nano-complexes with sizes less than 100 nm as shown in SEM images. TEM images revealed that the MNPs are well dispersed in the complexes of CPPs/pGL3, CPPs/SCO, and CPPs/siRNA. MNPS are less aggregated in the complexes of PF14/siRNA compared to the complexes of CPPs/pGL3 and CPPs/SCO. The synthesized MNPs had a positive zeta potential.

We investigated the complexes transfection ability of CPPs/pGL3/MNPs (CPPs; PF220, PF221, PF222, PF223, and PF224) in Hela cells. We measured the luminescence intensities after overnight treatment. The statistical analysis applying a two-way ANOVA test of CPPs/pGL3/MNPs (CPPs; PF220, PF221, PF222, PF223, PF224) presents no significant changes for PF220 or PF224. However, complexes of CPPs/pGL3/MNPs (CPPs; PF221, PF222, PF223) present higher efficiency (2–100 folds) compared to the similar CPPs/pGL3 without

MNPs. Splice correction oligonucleotide (SCO) assay was used to evaluate the transfection efficiency. All the results demonstrate that the involvement of MNPs increases the effectiveness of the PF14/SCO complexes. The SCO activity was improved by four times for PF14/SCO when MNPs was integrated into the complexes. The delivery of siRNA against the luciferase mRNA was investigated. PF14/siRNA/MNPs displayed significant down-regulation of the luciferase activity compared to PF14/siRNA with the same concentration.

The cellular uptake through Scavenger class A (SCARA) was investigated. HeLa cells were treated with small molecules inhibitors for SCARA (Dextran sulfate (Dex), polyinosinic acid (Poly I) or fucoidin (Fuc)). Moreover, their respective controls, e.g. structurally similar compounds (Chondroitin sulfate (Chon), polycytidylic acid (Poly C) or galactose (Gal)) before treatment with PF14/SCO/MNPs complexes. The controls Chon, Poly C, and Gal, lack affinity for SCARA. The SCO activity achieved by PF14/MNPs transfection is significantly reduced by using either inhibitor. The analogous inhibitor controls display no significant inhibition of the SCO activity. fucoidin (Fuc) and Dextran sulfate inhibit SCO activity mediated by PF14/SCO/MNPs transfection by more than 90%.

## 4.3. Paper III

TEM images of graphene oxide (GO) and GO/ONs/CPPs show a particle size of 100 nm. GO has negative zeta potential − 25 mV. The FT-IR spectrum of GO indicates the presence of various oxygen-containing functional groups in the GO structure including epoxide, carboxyl, and C–OH. FT-IR spectra were recorded showing the chemical covalent bonding between GO and CPPs (PF14 and PF221). The recording of a peak assigned to hydroxyl (namely phenol, C–OH) groups proves there are covalent bonding between GO and PF14 or PF221. Furthermore, the complexation of GO/CPPs (PF14 or PF221) with SCO are proved using FT-IR. The presence of SCO in the assembled vector with GO/CPPs (PF14 or PF221) is approved from the peaks of the deoxyribose region and stretching vibration of the phosphate groups in SCO. The functionalized GO/ONs/CPPs conserve the lamellar structure of GO. The analysis reveals a definite dark contrast of GO nanosheets.

GO/PF14 displays the structure of core-shell for pGL3 and siRNA. The modification of GO with ONs (pGL3, SCO, or siRNA) and CPPs (CPPs; PF14 or PF221) preserve the particle size of GO nanoparticles (133 nm). SEM analysis proves no change of the GO morphology. GO/siRNA/PF221 complexes display well-defined spherical particles. Energy dispersive X-ray (EDX) spectroscopy verifies the presence of the ONs in the complexes.

Transfection of HeLa cell using pGL3 Luciferase was examined. GO/pGL3 performs no gene transfection. GO/PF14/pGL3 produces an increase of the plasmid transfection by ~ 2 folds compared to pGL3/PF14. GO/pGL3/PF221 shows a 2.5-fold increase in transfection efficiency compared to pGL3/PF221. GO/SCO/PF14 transfection promotes >25-fold increase in splice correction activity compared to PF14/SCO. The mixture of GO/SCO provides no splice correction. The transfection using GO/SCO/PF221 shows an enhancement of the splice correction activity by ~ 17 folds. For studying cellular uptake through SCARA route, HeLa cells were treated with SCARA inhibitors before the transfection of GO/SCO/PF14 complexes. SCO activity mediated by GO/PF14 is strongly inhibited using the SCARA inhibitors. On the other hand, there is no influence on SCO activity for the controls.

## 4.4. Paper IV

We performed RNA sequencing analysis to investigate the influences of CPPs on the gene expression of HeLa cells. We used PF14 as a model CPP and analyzed the pattern of gene expression in cells treated with CPP compared to that of untreated cells. Moreover, we examined the impact of cargo molecule on the gene expression. We analysed the gene expression pattern in cells treated with PF14 complexed with cargo (PF14/SCO) to cells treated with PF14 and untreated cells. Our RNA sequencing data revealed the gene expression differences in case of treatment with PF14 and PF14/SCO. There were 292 significant genes differentially expressed in PF14 treatment and 934 genes in PF14/SCO complex. We used Ingenuity Pathway (IPA) interpretation to assign genes with significant expression changes in the relevant pathways. Based on the results of IPA analysis, PF14 has influenced multiple pathways regulating autophagy pathway.

After RNA sequencing, we decided to use qPCR to verify several of the most differentially expressed genes. The genes were chosen according to their potential to influence the autophagy due to the possible function of autophagy pathway in the control of the transfection process. The qPCR results enabled us to determine the cycle threshold of gene amplification. These cycle thresholds were then examined using the cycle threshold of the reference genes compared to untreated controls. Expression of 26 autophagy-related genes was analyzed. In the PF14 treatment NCOA7, APOBR, CTGF, PTK2, IGFBP1, PTGER4 and HRH1 expression was upregulated by at least two folds.
Furthermore, data shows 4-folds improvement for CTGF, NCOA7, and APOBR expression. On the other hand, ULK1, FOXJ2, ATG14, PIK3R3, and SESN2, revealed downregulation of expression by at least 0.5-fold changes. LDLR expression displayed a remarkable down-regulation by ten times. For PF14/SCO complex treatment experiments, we got an entirely distinct profile pattern with essentially down-regulation of the autophagy-related genes. These variations in the gene expression regulation profile can be a result of the structural differences among nanoparticle developed by cationic molecule and the complex composed of cationic and anionic molecules.

We treated HeLa cells with ligands that modulate autophagy pathway before we did PF14/SCO transfection. These ligands are acknowledged to activate or inhibit distinct proteins in the pathway. We chose the proteins targeted with ligands depending on the selected genes from the pathway analysis. This choice covered protein having a potential to influence autophagy based on the pathway analysis. CTGF inhibitor and focal adhesion kinase (FAK) inhibitor diminished 75% of the splice correction activity.
Furthermore, HMG-CoA reductase inhibitor and Prostaglandin E2 reduced 60% of the splice correction activity. Also starvation as an autophagy inducer significantly decreased the splice correction activity. However, splice correction efficacy was enhanced with ligand mTOR activator and TLR4 inhibitor. Moreover, the β-adrenoceptor antagonist increased the splice correction activity by 5-fold.

# 5. Discussion

Gene therapy using therapeutic agents such as ONs is usually limited due to cell charges, or nuclease degradation. Cell-penetrating peptide-based vectors as delivery vectors for the gene therapy are promising due to several reasons compared to viral and nonviral vectors. The combination of CPPs and inorganic nanoparticles is promising to overcome some of the challenges for CPPs. Nanoparticles increase the gene delivery efficiency and may offer possible targeting tools.

## 5.1. Design and validation of new cell-penetrating peptides

In the first paper, new cell-penetrating peptides were designed and tested using FQSAR prediction model constructed based on data generated from the earlier studies on PepFect (PF-20-28)[186]. Among different CPPs, PF 21 showed the highest biological activity in the former model, so we used it as a control. Statistical analysis revealed that PepFect 220 and PF 221 were significantly more efficient in delivering plasmids within the cells than PF 21. PepFect 221 shows high transfection for plasmid transfection compared to PepFect 224 peptide shows similar efficiency as PepFect 21. These results indicate a strong correlation with our model, where PepFect 220 and 221 were predicted to produce the highest biological activity.
Interestingly, the transfection efficiency is independent of the CPPs amphipathicity. The synthesized peptides have been investigated experimentally for PF 220, 221 and 224 for charge ratio 3. Though, the predicted biological activity for peptides PF 122 and 123 showed approximately 3 log unit's deviation from the observed values.

## 5.2. CPPs/iron oxide ($Fe_3O_4$) [ magnetic nanoparticles (MNPs)] for oligonucleotide delivery

In paper II[185], we used MNPs to be incorporated in the CPPs assembly with ONs to formulate more efficient gene delivery vector with magnetic targeting ability. TEM images are used to figure out the particle sizes of the formed complexes. TEM images of the pristine MNPs show particle size of 10 nm with average particle size 6.4 nm. MNPs display superparamagnetic characteristics superparamagnetic iron oxide (SPIO)[187]. The particle size was confirmed using SEM images. MNPs have positive surface charge (+2.4 mV) according to the zeta potential measurements. The low values of zeta potential (+2.4 mV) indicate that the colloidal of MNPs is unstable (stable colloidal solutions have a zeta potential of ±30 mV). The absence of coating agents or stabilizing agents renders the colloidal solution of MNPs unstable. The stability of the bare MNPs could be improved via the conjugation with CPPs and ONs.

The chemical structure and the length of the CPPs affect the morphology and the particle size of the formed nanocomplexes. PF 220/SCO/MNPs and PF 221/pGL3/MNPs show big spherical nanoparticles due to self-assembly of the small nanoparticles (100-150 nm) consisting of the three components (CPPs, ONs, and MNPs) via noncovalent electrostatic and hydrophobic interactions. Various CPPs have different chemical and physical properties. Thus they interact differently with the same ONs (pGL3, SCO, and siRNA). These interactions influence the physicochemical features of the nanocomplexes and eventually its biological efficacy. The zeta potentials of the CPPs/pGL3, PF14/siRNA, and CPPs/SCO complexes with MNPs show that the MNPs are impeded inside the complexes.

The efficacy of the developed complexes for ONs delivery was investigated. Plasmid transfection assay complexes of CPPs/pGL3/MNPs (PF221, PF222, PF223) show higher transfection efficiency compared to the corresponding CPPs/pGL3 without MNPs. The splice correction assay shows high cell transfection using CPPs/SCO/MNPs complexes compared to the corresponding complexes without MNPs. The amount of MNPs displayed significant influence on SCO delivery efficiency in a concentration-dependent

manner with pal shape activity pattern. Data shows that MNPs increase the cell transfection of PF14/SCO by 4-fold.
In the small interfering RNA (siRNA) assay, knockdown of luciferase gene expression using siRNA with and without MNPs was also examined. The delivery of siRNA generates degradation of the luciferase mRNA that leads to a reduction in the luminescence signal. PF14/siRNA/MNPs presented significant down-regulation of the luciferase expression compared to PF14/siRNA transfection. These results show that MNPs offer a considerable enhancement for the siRNA transfection. The high efficiency of PF14/siRNA/MNPs may be due to the high tendency to develop stable suspension as demonstrated by the anionic zeta potential.

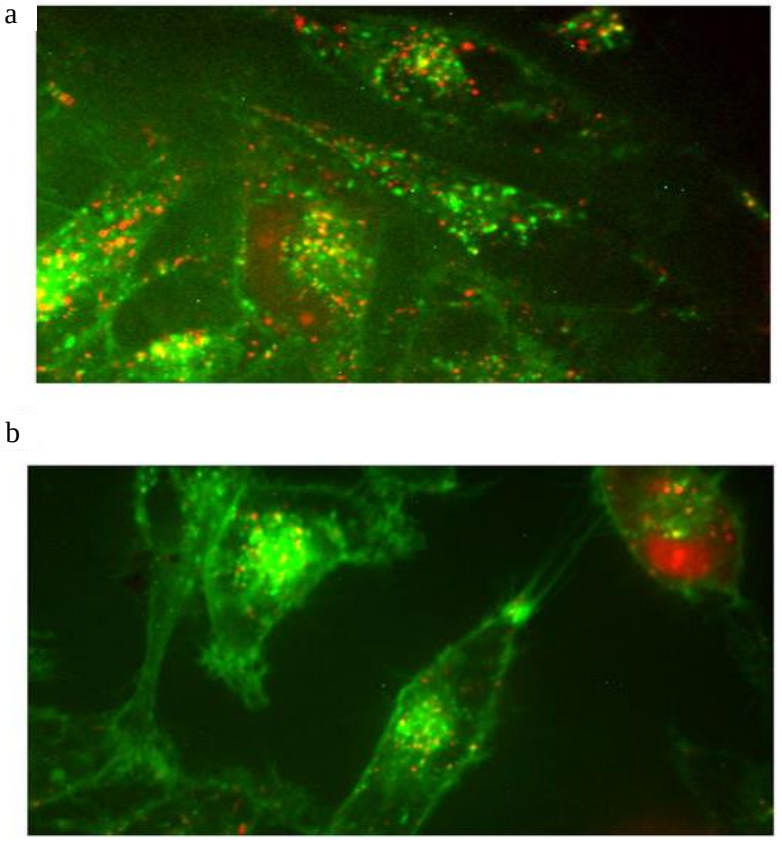


*Figure 3: Confocal microscope images of complexes uptake in Hela cells a) PF14SCO/MNPs b) PF14/SCO. The image is adapted with permission from Ref.185. (Paper II).*

The mechanism of cell uptake for PF14/SCO/MNPs was investigated using scavenger class A, and confocal microscopy (Figure 4). The cell transfection for ONs take place via several pathways including endocytosis, and scavenger receptor class A (SCARA) mediated endocytosis. Among these mechanisms, energy-independent translocation, endocytosis and scavenger receptor class A (SCARA) mediated endocytosis may be the reasonable explanations of the cellular uptake of these complexes. SCARA is a pattern recognition receptor with affinity for anionically charged particles. Also, it can bind and endocytose acetylated low-density lipoprotein[188]. SCARA inhibitors significantly reduced the splice correction activity. These measurements reinforce the high influence of scavenger receptor A in the cellular uptake of PF14/SCO/MNPs.

The internalization of these complexes into the cell was confirmed using confocal microscopy images (Figure 4) that show the presence of the ONs inside the cell. ONs are frequently trapped in endosomes which is vesicular structures inside the cell was observed as punctate structures. The activity improves with the rise in the percentage of the nucleic acids endosomal escape. This improvement can be realized using delivery vectors such as CPPs or CPPs/MNPs. The staining patterns of cells transfected with PF14-Alexa 568-705ASO complexes integrating MNPs revealed little variation compared to cells transfected with control complexes without MNPs. Therefore, the MNPs produced no change in the cellular uptake compared to the standard CPPs/ONs complexes. Despite, the new vectors with MNPs have higher transfection efficacy, showing that a more significant fraction of ONs can escape vesicular confinement. A study using electron tomography of intracellular trafficking of SPIO covalently conjugated with transactivating transcriptional activator (TAT) peptides originated from HIV-1 proteins proved the internalization of this complex into the cell[189].

Our system using MNPs offered several advantages. The MNPs improved the nucleic acid efficiency. PF14/SCO/MNPs shows 4-folds higher efficacy compared to PF14/SCO complexes. The new vectors efficacy may be enhanced additionally by activation using a magnetic field or thermal energy. CPPs/siRNA/MNPs encapsulated in liposomes displayed higher potency after activation using magnetic and thermal[190]. Therefore, we suppose that the efficiency of these complexes can be additionally improved using activation via a magnetic field, thermal, or infrared laser. The physio-chemical features of MNPs enhanced

the water-solubility and stability of the newly formed vectors. The small size of MNPs allowed efficient adsorption potential for CPPs/ONs complexes.

## 5.3. Graphene oxide (GO) nanosheets as a platform for hybrid CPP vector for oligonucleotide delivery

To proceed with the integration of nanoparticles to direct the self-assembly of our peptide-based delivery vectors, I used GO in paper III. GO was selected based on its unique physio-chemical properties. TEM image of the dispersed GO sheets shows a particle size of 100 nm. The zeta potential of GO is − 25 mV. The negative zeta potential of GO nanosheets is due to the presence of oxygenic functional groups including carboxyl, epoxy, hydroxyl, and carbonyl groups. The value of zeta potential shows that the GO produces a stable dispersion. The negative charge of GO sheets improves the modification with the positively charged such as cell penetrating peptides via electrostatic interactions. The surface of the GO nanosheets allows efficient and spontaneous protein adsorption[140]. It was published that the epoxide moieties on the GO sheets enable covalent bonds formation with lysine units (K) of the protein[140].

Based on the amino acid sequences of PF14, and PF221 they can be directly adsorbed and form covalent bonds with the epoxide functional groups of the GO sheets. FTIR spectra were recorded to approve the chemical bonding between the GO and CPPs (PF14 and PF221). A band at 1070 $cm^{-1}$is assigned to hydroxyl (namely phenol, C–OH) which confirm that there are covalent interactions between GO and PF14 or PF221[140].The complexation of GO, CPPs (PF221 or PF14) with oligonucleotides (pGL3, SCO or siRNA) is further approved from the zeta potential.

GO/pGL3/PF221, GO/siRNA/PF221, GO/pGL3/PF14, and GO/siRNA/PF14 show negative zeta potential values. On the other hand, GO/SCO/PF14 and GO/SCO/PF14 complexes are cationic. GO improve the CPPs/ONs binding as well as the hydrophilicity and dispersibility. The morphology of GO/ONs/CPPs (CPPs, PF221 or PF14; ONs, pGL3, SCO, or siRNA) complexes were investigated using TEM

images. The complexes of GO/ONs/CPPs preserve the lamellar structure of the pristine GO. TEM of the complexes display a dark contrast of GO nanosheets, indicating that the complexes of CPPs/ONs localized on the surface of the GO. GO/PF14 shows the formation of core-shell for siRNA and pGL3. It was published that single-stranded DNA (ss-DNA) macromolecules could be efficiently immobilized on the surface of graphene layers by π-π interactions connecting the hexagonal basal plane of GO and the aromatic bases of ss-DNA[191]. The assembly of GO with ONs (pGL3, SCO, or siRNA) and CPPs (PF221 or PF14) maintained the particle size of GO nanoparticles. The newly formed vectors have smaller particle sizes compared to the corresponding complexes without GO (i.e. CPPs/ONs)[36]. The aggregation tendency of CPPs/ONs results in the generation of microparticles (> 500 nm). The large particles of CPPs/ONs decrease the cellular uptake and may induce cytotoxicity. On the other hand, the integration of GO with extensive surface areas regulate the complexation and may limit the aggregation. In the same context, it was published that GO can be used as a modulator against protein misfolding and aggregations[192]. SEM analysis reveals no change in the GO morphology. GO/siRNA/PF221 complexes present the synthesis of well-defined self-assembled spherical particles. Energy dispersive X-ray (EDX) spectroscopy proves the presence of the ONs in the newly designed vectors.

GO/pGL3/CPPs (PF14 or PF221) were used to transfect HeLa cell using pGL3 Luciferase expressing plasmid. GO/PF14/pGL3 significantly improved the plasmid transfection compared to pGL3/PF14. Also, PF221 based GO vector for plasmid delivery GO/pGL3/PF221 shows an increase in transfection compared to pGL3/PF221. Cellular transfection of SCO using PF14 gives higher efficacy compared to the lipid-based vector Lipofectamine™ 2000 (LF2000) and persists active in serum[36]. GO/SCO/PF14 transfection demonstrates a superior improvement in splice correction activity compared to PF14/SCO.
Furthermore, the cellular transfection of GO/SCO/PF221 enhanced the splice correction activity significantly. The extracellular nuclease-mediated degradation of siRNA limits the cellular transfection of siRNA. Therefore, new vectors of GO modified cell penetrating peptides of PF221 and PF14 were designed. GO/siRNA/PF14, and PF14/siRNA show down-regulation of the investigated cells. GO gives no dramatic increases in the cellular transfection.

To investigate the cellular uptake of GO/SCO/PF14; scavenger receptor A (SCARA) role in the uptake process was studied. SCARA mediated endocytosis is a possible cellular uptake pathway for anionic species. HeLa cells were treated with SCARA inhibitors compared to their homologous controls before the transfection of GO/SCO/PF14 complexes. SCO activity produced by GO/SCO/PF14 transfection is significantly reduced by using the investigated SCARA inhibitors. On the other hand, there is no decrease in SCO efficacy for the controls treatments. These measurements show that the cellular uptake of GO/SCO/PF14 demands scavenger receptor A[193]. Confocal microscopy reveals the cellular delivery of PF14/SCO and GO/SCO/PF14. Nanocomplexes of PF14/SCO with and without GO undergo cellular localization. This investigation reveals that GO/SCO/PF14 proposes direct passage via endocytosis through the membrane system and escaping from the endosome[194]. One of the significant trends for the future is to investigate why GO/CPPs have higher efficacy compared to CPPs.

## 5.4. Autophagy pathway is involved in the cellular trafficking of peptide-based transfection

In paper IV[195], I investigated the cellular trafficking for PF14 transfection system as a model of peptide-based delivery using a transcriptomics approach. Aiming at revealing pathways involved in regulating cellular phenomena in the model CPP transfection system uptake process. Autophagy is a sort of an innate immunity pathway that is essential for degradation of misfolded proteins, dysfunctional cellular organelles, and pathogens. Autophagy is stimulated in nanoparticles transfection typically by pattern recognition receptors[196].
In paper IV, I reported that the model CPP transfection system induced autophagy induction (Figure 5).

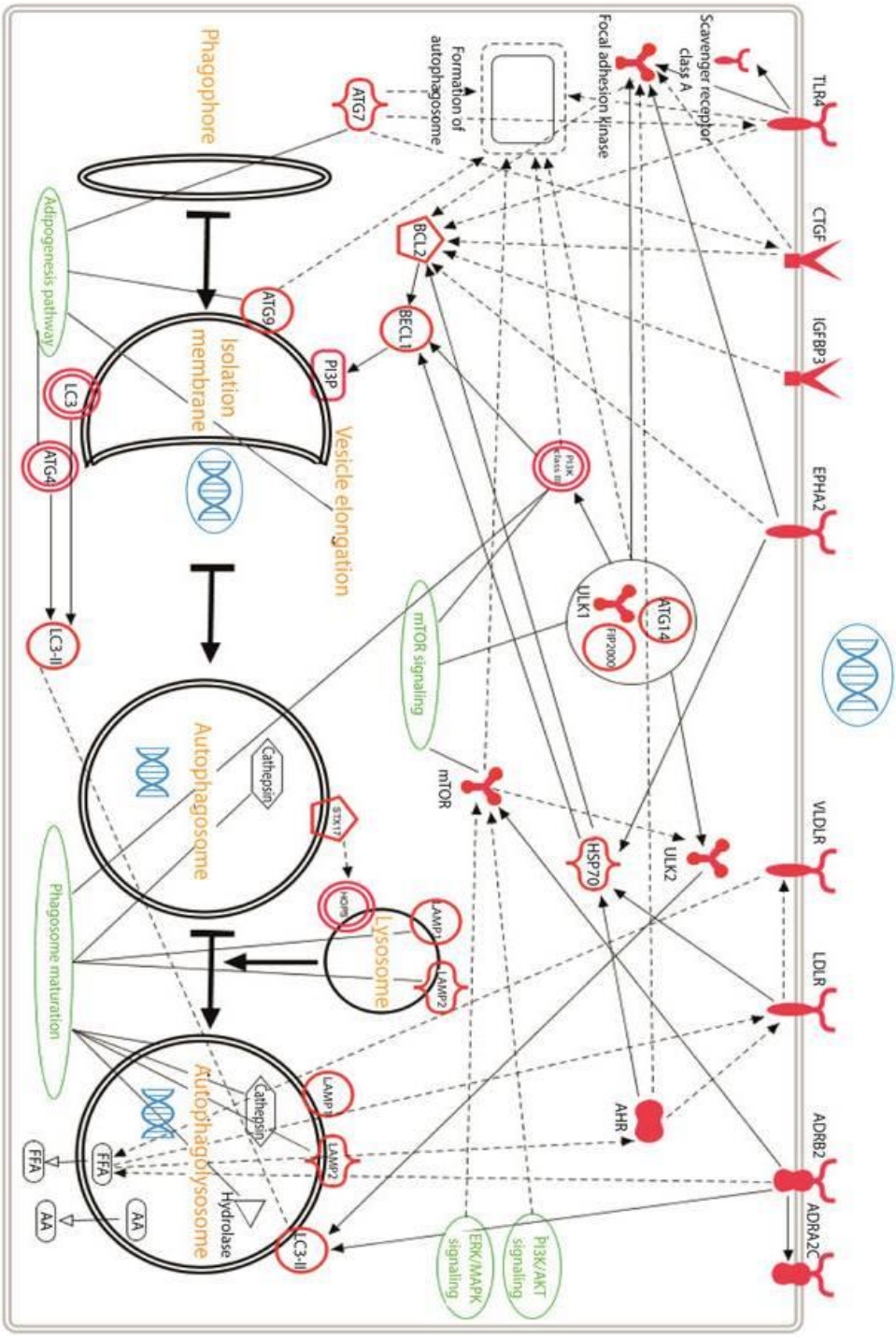


*Figure 4: Autophagy signalling pathway induced by CPP transfection. The image is adapted with permission from Ref.195. (Paper IV).*

I found that TLR4 is involved in the autophagy induced by PF14 and it is transfection system as I measured a significant increase in splice correction activity in the cells after inhibiting TLR4. This improvement in splice correction is in agreement with the approved role of TLRs in the non-canonical recruitment of Atg proteins to a single-membrane connected phagosome and phagophore formation step[197], which can confine the splice correction oligo that succeeded in the endosomal escape process. It has been reported that nanoparticles are trapped into autophagosomes, effectively separated from the cytoplasm, diminishing the relative toxicity and supporting in reducing cellular tension[198]. Induction of autophagy pathway has been first shown for the uptake of cationic polyplexes, silica, lipoplexes, dendrimers, gold nanoparticles and iron oxide[199–203]. In paper IV I show that positive charged CPP and PF14 complexed with oligonucleotide are inducing autophagy during their transfection process. Besides, autophagy can be advantageous for minimizing particles cytotoxicity; it can be restricting to cargo delivery, as in our CPP model of transfection, where the isolation of PF14 and its transfection system in autophagosomes and their degradation in autolysosomes decrease the splicing correction efficacy. If nucleic acid transfection system is mostly transported to autophagic organelles, only a limited amount of the cargo is transferred to the target cellular compartment; this is critically restricting efficiency and initiating to demand higher doses for treatment which can influence toxicity and cellular tension. In agreement with Roberts et al. showed that polyplex made of plasmid DNA and a polymer (JetPRIME, component unknown) was endocytosed and isolated in cellular tubulovesicular autophagosomes. They revealed that polyplex-mediated gene delivery was inducing autophagosomes generation, suggesting that autophagy can be a barrier to the gene delivery[204].

Chaperone-mediated autophagy is a distinct class of autophagy which regulates chaperone proteins and lysosomal receptors to transport marked proteins within the lysosomes, where degradation process occurs[205]. Marked proteins display a pentapeptide motif (KFERQ) and are therefore selectively recognized by the cytosolic chaperone Hsc70; that assists marked protein transportation to the lysosomes[206]. Moreover, HSP70 inhibitors are suppressing autophagy[207], so I used pifithrin-μ an HSP70 inhibitor which significantly enhanced the splice correction activity. Additional docking investigation revealed a possible binding between the PF14 peptide and the Hsc70. In wild-type macrophages, focal adhesion kinase (FAK) is at the surface of the Salmonella-containing

vacuole, starting the Akt-mTOR axis signalling and blocking of the autophagy induction. In FAK-deficient macrophages, Akt/mTOR signalling is suppressed, and autophagic isolation of intracellular bacteria is increased, leading to a significant increase of bacteria degradation[208]. In our results, FAK inhibition reduced the splice correction activity that is fitting with distinct autophagic degradation of the SCO comparable to the data of salmonella degradation in FAK-deficient macrophages.

Concerning mTOR pathway, to avoid autophagic degradation of our model of peptide transfection system, I activated mTOR pathway that significantly improved splice correction efficacy of our model vector, in agreement with the central role of mTOR in autophagy inhibition. Reports of the mTOR pathway association with several nanoparticles treatments have been shown to downregulate the mTOR pathway[209]. The β2-adrenergic receptor is a crucial regulator of autophagy[210], and I revealed that β2 antagonist makes a significant increase in the splice correction activity. Furthermore, autophagy initiation by atorvastatin[211] reduced our model vector-mediated splice correction activity. Prostaglandin E2 (PGE2) stimulates autophagy[212], and it showed an efficient reduction of splice correction.

# 6. Conclusions

The optimization of gene therapy for clinical purposes, including nucleic acid delivery to manage genetic disorders, has been limited by barriers to delivery. The shortage of data regarding the gene expression profiles describing the intracellular signalling pathways that are controlling the transfection process restricts the ability to design optimal delivery vectors. This thesis is a step to determine the molecular basis for efficient nucleic acid delivery and to apply that data to design effective nucleic acid delivery vectors. Developing efficient nucleic acid delivery vector needed to evaluate the impacts of the delivery systems individual elements including the peptide sequences on the delivery efficacy. The thesis showed strategies to integrate magnetic nanoparticles and graphene oxide nanosheets as new co-carrier for ON delivery. They showed enhancement of the self-assembly of the nucleic acid and offered superior improvement in their biological effects.
Furthermore, to determine the cellular uptake pathways of the nucleic acid delivery vectors, I investigated gene expression profiles of transfected cells. I reveal and confirm the role of autophagy pathway in regulating the transfection process. Therefore, with a refined description of gene expression profiles of several transfection systems, further optimized non-viral delivery vectors based on the analysis of the signalling pathways can be designed to facilitate therapeutic applicability.

I described a complete cycle for the development of novel cell-penetrating based delivery vectors. The thesis included logical prediction based on fragmentation of former peptides and design of a set of novel peptides to their synthesis and biological uptake. The FQSAR models were efficient in predicting peptides with the more significant biological activity than the published PF 21.

I demonstrated the development of new nanoplatforms for ON delivery. Hybrid ONs transfection vectors using magnetic nanoparticles and CPPs have been developed for cellular delivery of plasmid (pGL3), SCO and siRNA. Magnetic nanoparticles enhanced the biological efficacy compared to traditional CPPs/pGL3, CPPs/SCO, and CPPs/siRNA

complexes. PF14/SCO/MNPs displayed an improved biological activity (up to 4 times) compared to the PF 14/SCO complexes. This thesis showed several strategies for ONs transfection using magnetic nanoparticles and GO. The conjugation of GO and CPPs significantly enhances the cellular ONs transfection of pGL3 and SCO. The influence of the negative zeta potential and large surface area of GO improves the complexation of CPPs/ONs, inhibited aggregation and therefore gave a smaller size of these assemblies. GO/ONs/CPPs (PF 221 or PF 14) gave 2.1–2.5 and > 10–25 fold increase of the biological efficiency for pGL3 and SCO, respectively. The transfection efficacy depends on the concentration of GO. GO mediated CPPs/ONs vectors can be beneficial for the development of clinically safe and economically manageable ONs delivery. It could be used for in vivo investigations to deliver ONs to targeted tissues and promote their activity via focusing near infrared on the target tissues.

I demonstrated the autophagy induction and cellular effects triggered by CPP transfection vector in basal cell signalling. The autophagy induced by the transfection is a primary cellular defence pathway against the transfection vector, so it reduced the transfection efficiency by degrading the transfection vectors. This data about the molecular basis of the transfection process is valuable for the design of efficient nucleic acid delivery vector. PF 14 as a model transfection system is demonstrating the necessary capacity to deliver nucleic acid joined with non-toxic autophagy initiation, as a combinatory therapy strategy.

# 7. Acknowledgment

I thank my God (Allah) the most merciful for his guidance and his innumerable blessings for me to the right path.
I thank my supervisor Prof. Ülo Langel for the remarkable support, continuous guidance, motivation for creativity and innovation, encouraging new and wild hypothesis and evolving it.
Thanks to the Swedish Cancer Foundation, the Swedish Governmental Agency for Innovation Systems (VINNOVA) and the Swedish Research Council (VR) for funding our research.
I thank my co-supervisor Prof. Anders Undén. Also, I thank Prof. Einar Hallberg, Prof. Bengt Mannervik, Prof. Anna-Lena Ström, and all the professors in the department for their collaborations and support. I thank Prof. Xiaodong Zou and Dr. Hani N. Abdelhamid for the fruitful collaborations. I thank Prof. Ahmad Settin for introducing me to Genetics and his supervision in my master degree and my first Ph.D. I thank Prof. Tarek Salem for his help in my first Ph.D. I thank Prof. Ahmed Ali for his supervision in my first Ph.D.
I thank all my group members past and present, Thank you Kareim for introducing me to Sweden even before I came to it, and for the continuous scientific and social advice. Thank you, Mattias, for introducing me to the CPP field, being open-minded for all hypothesis with kind help in dedicated planning involving all possible controls, the intelligent discussions scientific and philosophical. Thank you, Jakob, for sharing the QSAR project with me and your help in it. Thank you, Maxime for current help in projects. Thank you, Carmine, for help in teaching the peptide synthesis lab. Thank you Kaido for all the successful collaborations we have together. Thank you, Henrik, for all the technical and quality standardization advice. Thank you, Anders, for your multicultural activity and sense of humor. Thank you, Daniel, for help in teaching the proteomics lab. Thank you, Ying, for sharing the courses materials. Thank you Tõnis for the discussions and company in teaching labs. Thank you, Ricardo, for the help with the microscopes. I thank Marie-Louise for the help.

I thank my colleges: Rania, Staffan, Jonas, Ajayi, Anna, Aslam, Balaje, Birgitta, Dan, Elena, Frida, Hakim, Helena, Jessica, Kalicharan, Kristin, Kristina, Mehedi, Preeti, Santosh, Veronica.

I thank my friends: Hani Mobarak, Ahmed Ramzy, Ahmed Etman, Ramy Helal, Medhat Khalil, and Hatem El-Mongy.

I deeply thank my mother and father for their unlimited care, help, and support for me since I existed, I thank my sister Dr. Heba and my brothers Dr. Ibrahim and Dr. Ahmed for their help and support. I thank my wife and my kids.

# 8. References


1. Kohman, R. E., Kunjapur, A. M., Hysolli, E., Wang, Y. & Church, G. M. From Designing the Molecules of Life to Designing Life: Future Applications Derived from Advances in DNA Technologies. *Angewandte Chemie - International Edition* **57,** 4313–4328 (2018).
2. Verma, I. M. & Somia, N. Gene therapy-promises, problems and prospects. *Nature* **389,** 239–42 (1997).
3. Rinaldi, C. & Wood, M. J. A. Antisense oligonucleotides: the next frontier for treatment of neurological disorders. *Nat. Rev. Neurol.* **14,** 9 (2017).
4. Mehier-Humbert, S. & Guy, R. H. Physical methods for gene transfer: Improving the kinetics of gene delivery into cells. *Advanced Drug Delivery Reviews* **57,** 733–753 (2005).
5. Naldini, L. Gene therapy returns to centre stage. *Nature* **526,** 351–360 (2015).
6. Powell, A. B., Williams, K. & Cruz, C. R. Y. Gene-modified, cell-based therapies—an overview. *Cytotherapy* **18,** 1351–1359 (2016).
7. Young, L. S., Searle, P. F., Onion, D. & Mautner, V. Viral gene therapy strategies: from basic science to clinical application. *J. Pathol.* **208,** 299–318 (2006).
8. Wang, X. & Rivière, I. Clinical manufacturing of CAR T cells: Foundation of a promising therapy. *Molecular Therapy - Oncolytics* **3,** (2016).
9. Senior, M. After Glybera's withdrawal, what's next for gene therapy? *Nat. Biotechnol.* **35,** 491 (2017).
10. Naldini, L. Ex vivo gene transfer and correction for cell-based therapies. *Nature Reviews Genetics* **12,** 301–315 (2011).
11. Wolff, J.A., Malone, R.W., Williams, P., Chong, W., Acsadi, G., Jani, A., Felgner, P. L. Direct gene transfer into mouse muscle in vivo. *Science (80-. ).* **247,** 1465–1468 (1990).
12. Houk, B. E., Hochhaus, G. & Hughes, J. a. Kinetic modeling of plasmid DNA degradation in rat plasma. *AAPS PharmSci* **1,** E9

(1999).
13. Lechardeur, D. *et al.* Metabolic instability of plasmid DNA in the cytosol: A potential barrier to gene transfer. *Gene Ther.* **6,** 482–497 (1999).
14. Narsinh, K. H. *et al.* Generation of adult human induced pluripotent stem cells using nonviral minicircle DNA vectors. *Nat. Protoc.* **6,** 78–88 (2011).
15. Hilchie, A. L., Wuerth, K. & Hancock, R. E. W. Immune modulation by multifaceted cationic host defense (antimicrobial) peptides. *Nature Chemical Biology* **9,** 761–768 (2013).
16. Winn, M., Fyans, J. K., Zhuo, Y. & Micklefield, J. Recent advances in engineering nonribosomal peptide assembly lines. *Nat. Prod. Rep.* **33,** 317–347 (2016).
17. Rhodes, C. A. & Pei, D. Bicyclic Peptides as Next-Generation Therapeutics. *Chemistry - A European Journal* **23,** 12690–12703 (2017).
18. Yin, H. *et al.* Non-viral vectors for gene-based therapy. *Nat. Rev. Genet.* **15,** 541 (2014).
19. Langel, Ü. *Cell-Penetrating Peptides*. *Methods in molecular biology (Clifton, N.J.)* **683,** (2011).
20. Illien, F. *et al.* Quantitative fluorescence spectroscopy and flow cytometry analyses of cell-penetrating peptides internalization pathways: Optimization, pitfalls, comparison with mass spectrometry quantification. *Sci. Rep.* **6,** (2016).
21. Walrant, A., Cardon, S., Burlina, F. & Sagan, S. Membrane Crossing and Membranotropic Activity of Cell-Penetrating Peptides: Dangerous Liaisons? *Acc. Chem. Res.* **50,** 2968–2975 (2017).
22. Guidotti, G., Brambilla, L. & Rossi, D. Cell-Penetrating Peptides: From Basic Research to Clinics. *Trends in Pharmacological Sciences* **38,** 406–424 (2017).
23. Kim, C. H., Lee, S. G., Kang, M. J., Lee, S. & Choi, Y. W. Surface modification of lipid-based nanocarriers for cancer cell-specific drug targeting. *Journal of Pharmaceutical Investigation* **47,** 203–227 (2017).
24. Green, M. & Loewenstein, P. M. Autonomous functional domains of chemically synthesized human immunodeficiency virus tat trans-activator protein. *Cell* **55,** 1179–1188 (1988).
25. Frankel, a D. & Pabo, C. O. Cellular uptake of the tat protein from human immunodeficiency virus. *Cell* **55,** 1189–1193 (1988).

26. Elliott, G. & O'Hare, P. Intercellular trafficking and protein delivery by a herpesvirus structural protein. *Cell* **88,** 223–233 (1997).
27. Joliot, A., Pernelle, C., Deagostini-Bazin, H. & Prochiantz, A. Antennapedia homeobox peptide regulates neural morphogenesis. *Proc. Natl. Acad. Sci.* **88,** 1864–1868 (1991).
28. Derossi, D., Joliot, A. H., Chassaing, G. & Prochiantz, A. The third helix of the Antennapedia homeodomain translocates through biological membranes. *J. Biol. Chem.* **269,** 10444–10450 (1994).
29. Pooga, M., Hällbrink, M., Zorko, M. & Langel, Ü. Cell penetration by transportan. *FASEB J.* **12,** 67–77 (1998).
30. Wender, P. A. *et al.* The design, synthesis, and evaluation of molecules that enable or enhance cellular uptake: Peptoid molecular transporters. *Proc. Natl. Acad. Sci.* **97,** 13003–13008 (2000).
31. Oehlke, J. *et al.* Cellular uptake of an α-helical amphipathic model peptide with the potential to deliver polar compounds into the cell interior non-endocytically. *Biochim. Biophys. Acta - Biomembr.* **1414,** 127–139 (1998).
32. Marks, J. R., Placone, J., Hristova, K. & Wimley, W. C. Spontaneous membrane-translocating peptides by orthogonal high-throughput screening. *J. Am. Chem. Soc.* **133,** 8995–9004 (2011).
33. Mäe, M. *et al.* A stearylated CPP for delivery of splice correcting oligonucleotides using a non-covalent co-incubation strategy. *J. Control. Release* **134,** 221–227 (2009).
34. Lehto, T. *et al.* A peptide-based vector for efficient gene transfer in vitro and in vivo. *Mol. Ther.* **19,** 1457–1467 (2011).
35. Andaloussi, S. E. L. *et al.* Design of a peptide-based vector, PepFect6, for efficient delivery of siRNA in cell culture and systemically in vivo. *Nucleic Acids Res.* **39,** 3972–3987 (2011).
36. Ezzat, K. *et al.* PepFect 14, a novel cell-penetrating peptide for oligonucleotide delivery in solution and as solid formulation. *Nucleic Acids Res.* **39,** 5284–5298 (2011).
37. Ezzat, K. *et al.* Solid formulation of cell-penetrating peptide nanocomplexes with siRNA and their stability in simulated gastric conditions. *J. Control. Release* **162,** 1–8 (2012).
38. Veiman, K. L. *et al.* PepFect14 peptide vector for efficient gene delivery in cell cultures. *Mol. Pharm.* **10,** 199–210 (2013).
39. Ziegler, A. Thermodynamic studies and binding mechanisms of

cell-penetrating peptides with lipids and glycosaminoglycans. *Advanced Drug Delivery Reviews* **60,** 580–597 (2008).
40. Zaro, J. L. & Shen, W. C. Cationic and amphipathic cell-penetrating peptides (CPPs): Their structures and in vivo studies in drug delivery. *Frontiers of Chemical Science and Engineering* **9,** 407–427 (2015).
41. Niidome, T. *et al.* Influence of lipophilic groups in cationic α-helical peptides on their abilities to bind with DNA and deliver genes into cells. *J. Pept. Res.* **54,** 361–367 (1999).
42. Milletti, F. Cell-penetrating peptides: Classes, origin, and current landscape. *Drug Discovery Today* **17,** 850–860 (2012).
43. Soomets, U. *et al.* Deletion analogues of transportan. *Biochim. Biophys. Acta - Biomembr.* **1467,** 165–176 (2000).
44. Scheller, A. *et al.* Structural requirements for cellular uptake of α-helical amphipathic peptides. *J. Pept. Sci.* **5,** 185–194 (1999).
45. Park, K. In vivo DNA delivery with NickFect peptide vectors. *Journal of Controlled Release* **241,** 242 (2016).
46. Hällbrink, M. & Karelson, M. Prediction of cell-penetrating peptides. in *Cell-Penetrating Peptides: Methods and Protocols* 39–58 (2015). doi:10.1007/978-1-4939-2806-4_3
47. Cheng, C. J., Tietjen, G. T., Saucier-Sawyer, J. K. & Saltzman, W. M. A holistic approach to targeting disease with polymeric nanoparticles. *Nature Reviews Drug Discovery* **14,** 239–247 (2015).
48. Abdelhamid, H. N. & Zou, X. Template-free and room temperature synthesis of hierarchical porous zeolitic imidazolate framework nanoparticles and their dye and CO 2 sorption. *Green Chem.* **20,** 1074–1084 (2018).
49. Abdelhamid, H. N. Lanthanide Metal-Organic Frameworks and Hierarchical Porous Zeolitic Imidazolate Frameworks: Synthesis, Properties, and Applications. (Stockholm University, 2017).
50. Gopal, J., Abdelhamid, H. N., Huang, J. H. & Wu, H. F. Nondestructive detection of the freshness of fruits and vegetables using gold and silver nanoparticle mediated graphene enhanced Raman spectroscopy. *Sensors Actuators, B Chem.* **224,** 413–424 (2016).
51. Abdelhamid, H. N. & Wu, H. F. Thymine chitosan nanomagnets for specific preconcentration of mercury (II) prior to analysis using SELDI-MS. *Microchim. Acta* **184,** 1517–1527 (2017).
52. Yang, Y. *et al.* A Zn-MOF constructed from electron-rich π-

conjugated ligands with an interpenetrated graphene-like net as an efficient nitroaromatic sensor. *RSC Adv.* **6,** 45475–45481 (2016).
53. Zou, X. *et al.* A series of highly stable isoreticular lanthanide metal-organic frameworks with tunable luminescence properties solved by rotation electron diffraction and X-ray diffraction. *Acta Crystallogr. Sect. A Found. Adv.* **72,** s136–s136 (2016).
54. Shastri, L., Abdelhamid, H. N., Nawaz, M. & Wu, H.-F. Synthesis, characterization and bifunctional applications of bidentate silver nanoparticle assisted single drop microextraction as a highly sensitive preconcentrating probe for protein analysis. *RSC Adv.* **5,** 41595–41603 (2015).
55. Gedda, G., Abdelhamid, H. N., Khan, M. S. & Wu, H.-F. ZnO nanoparticle-modified polymethyl methacrylate-assisted dispersive liquid–liquid microextraction coupled with MALDI-MS for rapid pathogenic bacteria analysis. *RSC Adv.* **4,** 45973–45983 (2014).
56. Abdelhamid, H. N. Delafossite Nanoparticle as New Functional Materials: Advances in Energy, Nanomedicine and Environmental Applications. *Mater. Sci. Forum* **832,** 28–53 (2015).
57. Yao, Q. *et al.* Series of Highly Stable Isoreticular Lanthanide Metal–Organic Frameworks with Expanding Pore Size and Tunable Luminescent Properties. *Chem. Mater.* **27,** 5332–5339 (2015).
58. Abdelhamid, H. N. & Wu, H.-F. Synthesis and characterization of quantum dots for application in laser soft desorption/ionization mass spectrometry to detect labile metal–drug interactions and their antibacterial activity. *RSC Adv.* **5,** 76107–76115 (2015).
59. Wu, H., Zhu, L. & Torchilin, V. P. pH-sensitive poly(histidine)-PEG/DSPE-PEG co-polymer micelles for cytosolic drug delivery. *Biomaterials* **34,** 1213–22 (2013).
60. Iqbal, M. N. *et al.* Mesoporous Ruthenium Oxide: A Heterogeneous Catalyst for Water Oxidation. *ACS Sustain. Chem. Eng.* **5,** 9651–9656 (2017).
61. Etman, A. S. *et al.* Facile Water-Based Strategy for Synthesizing MoO3– x Nanosheets: Efficient Visible Light Photocatalysts for Dye Degradation. *ACS Omega* **3,** 2193–2201 (2018).
62. Abdelhamid, H. N., Chen, Z.-Y. & Wu, H.-F. Surface tuning laser desorption/ionization mass spectrometry (STLDI-MS) for

the analysis of small molecules using quantum dots. *Anal. Bioanal. Chem.* **409,** 4943–4950 (2017).
63. Kumaran, S., Abdelhamid, H. N. & Wu, H.-F. Quantification analysis of protein and mycelium contents upon inhibition of melanin for: Aspergillus Niger: A study of matrix assisted laser desorption/ionization mass spectrometry (MALDI-MS). *RSC Adv.* **7,** 30289–30294 (2017).
64. Abdelhamid, H. N. & Wu, H.-F. Selective biosensing of Staphylococcus aureus using chitosan quantum dots. *Spectrochim. Acta - Part A Mol. Biomol. Spectrosc.* **188,** (2018).
65. Abdelhamid, H. N., Huang, Z., El-Zohry, A. M., Zheng, H. & Zou, X. A Fast and Scalable Approach for Synthesis of Hierarchical Porous Zeolitic Imidazolate Frameworks and One-Pot Encapsulation of Target Molecules. *Inorg. Chem.* **56,** 9139–9146 (2017).
66. Abdelhamid, H. N., Bermejo-Gómez, A., Martín-Matute, B. & Zou, X. A water-stable lanthanide metal-organic framework for fluorimetric detection of ferric ions and tryptophan. *Microchim. Acta* **184,** 3363–3371 (2017).
67. Abdelhamid, H. N. & Wu, H.-F. Gold nanoparticles assisted laser desorption/ionization mass spectrometry and applications: from simple molecules to intact cells. *Anal. Bioanal. Chem.* **408,** 4485–4502 (2016).
68. Abdelhamid, H. N., Talib, A. & Wu, H. F. One pot synthesis of gold – carbon dots nanocomposite and its application for cytosensing of metals for cancer cells. *Talanta* **166,** 357–363 (2017).
69. Petros, R. A. & Desimone, J. M. Strategies in the design of nanoparticles for therapeutic applications. *Nature Reviews Drug Discovery* **9,** 615–627 (2010).
70. Lee, J., Yang, J., Kwon, S. G. & Hyeon, T. Nonclassical nucleation and growth of inorganic nanoparticles. *Nature Reviews Materials* **1,** (2016).
71. Abdelhamid, H. N., Lin, Y. C. & Wu, H.-F. Magnetic nanoparticle modified chitosan for surface enhanced laser desorption/ionization mass spectrometry of surfactants. *RSC Adv.* **7,** 41585–41592 (2017).
72. Abdelhamid, H. N., Lin, Y. C. & Wu, H. F. Thymine chitosan nanomagnets for specific preconcentration of mercury (II) prior to analysis using SELDI-MS. *Microchim. Acta* **184,** 1517–1527 (2017).

73. H. N. Abdelhamid. Applications of Nanomaterials and Organic Semiconductors for Bacteria &Biomolecules analysis/ biosensing using Laser Analytical Spectroscopy. (National Sun-Yat Sen University, 2013). doi:etd-0608113-135030
74. Abdelhamid, H. N., Kumaran, S. & Wu, H.-F. One-pot synthesis of CuFeO2 nanoparticles capped with glycerol and proteomic analysis of their nanocytotoxicity against fungi. *RSC Adv.* **6,** 97629–97635 (2016).
75. Abdelhamid, H. N. Laser Assisted Synthesis, Imaging and Cancer Therapy of Magnetic Nanoparticles. *Mater. Focus* **5,** 305–323 (2016).
76. Gopal, J., Abdelhamid, H. N., Hua, P.-Y. & Wu, H.-F. Chitosan nanomagnets for effective extraction and sensitive mass spectrometric detection of pathogenic bacterial endotoxin from human urine. *J. Mater. Chem. B* **1,** 2463–2475 (2013).
77. Abdelhamid, H. N., Talib, A. & Wu, H.-F. Facile synthesis of water soluble silver ferrite (AgFeO2) nanoparticles and their biological application as antibacterial agents. *RSC Adv.* **5,** 34594–34602 (2015).
78. Abdelhamid, H. N. & Wu, H.-F. Facile synthesis of nano silver ferrite (AgFeO2) modified with chitosan applied for biothiol separation. *Mater. Sci. Eng. C. Mater. Biol. Appl.* **45,** 438–45 (2014).
79. Abdelhamid, H. N. & Wu, H.-F. Proteomics analysis of the mode of antibacterial action of nanoparticles and their interactions with proteins. *TrAC Trends Anal. Chem.* **65,** 30–46 (2014).
80. Haun, J. B., Yoon, T. J., Lee, H. & Weissleder, R. Magnetic nanoparticle biosensors. *Wiley Interdisciplinary Reviews: Nanomedicine and Nanobiotechnology* **2,** 291–304 (2010).
81. Yildiz, I. Applications of magnetic nanoparticles in biomedical separation and purification. *Nanotechnology Reviews* **5,** 331–340 (2016).
82. Mahmoudi, M. *et al.* A new approach for the in vitro identification of the cytotoxicity of superparamagnetic iron oxide nanoparticles. *Colloids Surfaces B Biointerfaces* **75,** 300–309 (2010).
83. Rajiv, S. *et al.* Comparative cytotoxicity and genotoxicity of cobalt (II, III) oxide, iron (III) oxide, silicon dioxide, and aluminum oxide nanoparticles on human lymphocytes in vitro. *Hum. Exp. Toxicol.* **35,** 170–183 (2016).
84. Pandey, R. K., Sundar, S. & Prajapati, V. K. Differential

expression of miRNA regulates T cell differentiation and plasticity during visceral leishmaniasis infection. *Front. Microbiol.* **7,** (2016).
85. Yu, J. *et al.* Multifunctional Fe5C2nanoparticles: A targeted theranostic platform for magnetic resonance imaging and photoacoustic tomography-guided photothermal therapy. *Adv. Mater.* **26,** 4114–4120 (2014).
86. Ju, Y. *et al.* Monodisperse Au-Fe2C Janus Nanoparticles: An Attractive Multifunctional Material for Triple-Modal Imaging-Guided Tumor Photothermal Therapy. *ACS Nano* **11,** 9239–9248 (2017).
87. Thorat, N. D. *et al.* Effective Cancer Theranostics with Polymer Encapsulated Superparamagnetic Nanoparticles: Combined Effects of Magnetic Hyperthermia and Controlled Drug Release. *ACS Biomater. Sci. Eng.* **3,** 1332–1340 (2017).
88. Wust, P. *et al.* Magnetic nanoparticles for interstitial thermotherapy - Feasibility, tolerance and achieved temperatures. *Int. J. Hyperth.* **22,** 673–685 (2006).
89. Johannsen, M. *et al.* Morbidity and quality of life during thermotherapy using magnetic nanoparticles in locally recurrent prostate cancer: Results of a prospective phase I trial. *Int. J. Hyperth.* **23,** 315–323 (2007).
90. Maier-Hauff, K. *et al.* Efficacy and safety of intratumoral thermotherapy using magnetic iron-oxide nanoparticles combined with external beam radiotherapy on patients with recurrent glioblastoma multiforme. *J. Neurooncol.* **103,** 317–324 (2011).
91. van Landeghem, F. K. H. *et al.* Post-mortem studies in glioblastoma patients treated with thermotherapy using magnetic nanoparticles. *Biomaterials* **30,** 52–57 (2009).
92. Liu, G. *et al.* N-Alkyl-PEI-functionalized iron oxide nanoclusters for efficient siRNA delivery. *Small* **7,** 2742–2749 (2011).
93. Borroni, E. *et al.* Tumor targeting by lentiviral vectors combined with magnetic nanoparticles in mice. *Acta Biomater.* **59,** 303–316 (2017).
94. Khanna, L., Verma, N. K. & Tripathi, S. K. Burgeoning tool of biomedical applications - Superparamagnetic nanoparticles. *J. Alloys Compd.* **752,** 332–353 (2018).
95. McBain, S. C. *et al.* Magnetic nanoparticles as gene delivery agents: Enhanced transfection in the presence of oscillating

magnet arrays. *Nanotechnology* **19,** (2008).
96. Fouriki, A. & Dobson, J. Oscillating magnet array-based nanomagnetic gene transfection of human mesenchymal stem cells. *Nanomedicine (London, U. K.)* **9,** 989–997 (2014).
97. Fouriki, A. & Dobson, J. Nanomagnetic gene transfection for non-viral gene delivery in nih 3t3 mouse embryonic fibroblasts. *Materials (Basel).* **6,** 255–264 (2013).
98. Liu, X. *et al.* Polyamidoamine dendrimer and oleic acid-functionalized graphene as biocompatible and efficient gene delivery vectors. *ACS Appl. Mater. Interfaces* **6,** 8173–8183 (2014).
99. Wang, C., Qiao, L., Zhang, Q., Yan, H. & Liu, K. Enhanced cell uptake of superparamagnetic iron oxide nanoparticles through direct chemisorption of FITC-Tat-PEG600-b-poly(glycerol monoacrylate). *Int. J. Pharm.* **430,** 372–380 (2012).
100. Cavalli, S. *et al.* Efficient γ-amino-proline-derived cell penetrating peptide–superparamagnetic iron oxide nanoparticle conjugates via aniline-catalyzed oxime chemistry as bimodal imaging nanoagents. *Chem. Commun.* **48,** 5322 (2012).
101. Harris, T. J. *et al.* Protease-triggered unveiling of bioactive nanoparticles. *Small* **4,** 1307–1312 (2008).
102. Ogbodu, R. O. & Nyokong, T. Effect of bovine serum albumin and single walled carbon nanotube on the photophysical properties of zinc octacarboxy phthalocyanine. *Spectrochim. Acta - Part A Mol. Biomol. Spectrosc.* **121,** 81–87 (2014).
103. Stankovich, S. *et al.* Graphene-based composite materials. *Nature* **442,** 282–286 (2006).
104. Geim, A. K. & Novoselov, K. S. The rise of graphene. *Nat. Mater.* **6,** 183–191 (2007).
105. Stoller, M. D., Park, S., Yanwu, Z., An, J. & Ruoff, R. S. Graphene-Based ultracapacitors. *Nano Lett.* **8,** 3498–3502 (2008).
106. Maier, S. A. Graphene plasmonics: All eyes on flatland. *Nature Physics* **8,** 581–582 (2012).
107. Liu, J. Charging graphene for energy. *Nat. Nanotechnol.* **9,** 739–741 (2014).
108. Kim, T. H., Lee, D. & Choi, J. W. Live cell biosensing platforms using graphene-based hybrid nanomaterials. *Biosensors and Bioelectronics* **94,** 485–499 (2017).
109. Heerema, S. J. & Dekker, C. Graphene nanodevices for DNA sequencing. *Nature Nanotechnology* **11,** 127–136 (2016).

110. Ashour, R. M. *et al.* Rare Earth Ions Adsorption onto Graphene Oxide Nanosheets. *Solvent Extr. Ion Exch.* (2017). doi:10.1080/07366299.2017.1287509
111. Abdelhamid, H. N. & Wu, H.-F. Reduced graphene oxide conjugate thymine as a new probe for ultrasensitive and selective fluorometric determination of mercury(II) ions. *Microchim. Acta* **182,** (2015).
112. Abdelhamid, H. N., Khan, M. S. & Wu, H.-F. Graphene oxide as a nanocarrier for gramicidin (GOGD) for high antibacterial performance. *RSC Adv.* **4,** 50035–50046 (2014).
113. Li, F., Yu, Y., Li, Q., Zhou, M. & Cui, H. A Homogeneous Signal-On Strategy for the Detection of *rpoB* Genes of Mycobacterium tuberculosis Based on Electrochemiluminescent Graphene Oxide and Ferrocene Quenching. *Anal. Chem.* **86,** 1608–1613 (2014).
114. Abdelhamid, H. N. & Wu, H.-F. Ultrasensitive, Rapid, and Selective Detection of Mercury Using Graphene Assisted Laser Desorption/Ionization Mass Spectrometry. *J. Am. Soc. Mass Spectrom.* **25,** 861–868 (2014).
115. Abdelhamid, H. N. & Wu, H.-F. Multifunctional graphene magnetic nanosheet decorated with chitosan for highly sensitive detection of pathogenic bacteria. *J. Mater. Chem. B* **1,** 3950–3961 (2013).
116. Abdelhamid, H. N. & Wu, H.-F. Synthesis of a highly dispersive sinapinic acid@graphene oxide (SA@GO) and its applications as a novel surface assisted laser desorption/ionization mass spectrometry for proteomics and pathogenic bacteria biosensing. *Analyst* **140,** 1555–1565 (2015).
117. Abdelhamid, H. N. & Wu, H.-F. A method to detect metal-drug complexes and their interactions with pathogenic bacteria via graphene nanosheet assist laser desorption/ionization mass spectrometry and biosensors. *Anal. Chim. Acta* **751,** 94–104 (2012).
118. Wu, B.-S., Abdelhamid, H. N. & Wu, H.-F. Synthesis and antibacterial activities of graphene decorated with stannous dioxide. *RSC Adv.* **4,** 3722 (2014).
119. Singh, D. P. *et al.* Graphene oxide: An efficient material and recent approach for biotechnological and biomedical applications. *Mater. Sci. Eng. C* **86,** 173–197 (2018).
120. Bagri, A. *et al.* Structural evolution during the reduction of chemically derived graphene oxide. *Nat. Chem.* **2,** 581–587

(2010).
121. Sun, X. *et al.* Nano-Graphene Oxide for Cellular Imaging and Drug Delivery. *Nano Res* **1,** 203–212 (2008).
122. C., W. *et al.* Gold nanoclusters and graphene nanocomposites for drug delivery and imaging of cancer cells. *Angew. Chemie - Int. Ed.* **50,** 11644–11648 (2011).
123. Depan, D., Shah, J. & Misra, R. D. K. Controlled release of drug from folate-decorated and graphene mediated drug delivery system: Synthesis, loading efficiency, and drug release response. *Mater. Sci. Eng. C* **31,** 1305–1312 (2011).
124. Liu, Z., Robinson, J. T., Sun, X. & Dai, H. PEGylated nanographene oxide for delivery of water-insoluble cancer drugs. *J. Am. Chem. Soc.* **130,** 10876–10877 (2008).
125. Zhao, X. *et al.* Interactive oxidation-reduction reaction for the in situ synthesis of graphene-phenol formaldehyde composites with enhanced properties. *ACS Appl. Mater. Interfaces* **6,** 4254–4263 (2014).
126. Wang, L., Zhang, Y., Wu, A. & Wei, G. Designed graphene-peptide nanocomposites for biosensor applications: A review. *Analytica Chimica Acta* **985,** 24–40 (2017).
127. Li, M., Yang, X., Ren, J., Qu, K. & Qu, X. Using graphene oxide high near-infrared absorbance for photothermal treatment of Alzheimer's disease. *Adv. Mater.* **24,** 1722–1728 (2012).
128. Shahnawaz Khan, M., Abdelhamid, H. N. & Wu, H.-F. Near infrared (NIR) laser mediated surface activation of graphene oxide nanoflakes for efficient antibacterial, antifungal and wound healing treatment. *Colloids Surf. B. Biointerfaces* **127C,** 281–291 (2015).
129. Hu, H., Tang, C. & Yin, C. Folate conjugated trimethyl chitosan/graphene oxide nanocomplexes as potential carriers for drug and gene delivery. *Mater. Lett.* **125,** 82–85 (2014).
130. Teimouri, M., Nia, A. H., Abnous, K., Eshghi, H. & Ramezani, M. Graphene oxide-cationic polymer conjugates: Synthesis and application as gene delivery vectors. *Plasmid* **84–85,** 51–60 (2016).
131. Tian, B., Wang, C., Zhang, S., Feng, L. & Liu, Z. Photothermally enhanced photodynamic therapy delivered by nano-graphene oxide. *ACS Nano* **5,** 7000–7009 (2011).
132. Feng, L., Zhang, S. & Liu, Z. Graphene based gene transfection. *Nanoscale* **3,** 1252 (2011).
133. Cao, X. *et al.* Functionalized Graphene Oxide with Hepatocyte

Targeting as Anti-Tumor Drug and Gene Intracellular Transporters. *J. Nanosci. Nanotechnol.* **15,** 2052–2059 (2015).
134. Yang, H. W. *et al.* Gadolinium-functionalized nanographene oxide for combined drug and microRNA delivery and magnetic resonance imaging. *Biomaterials* **35,** 6534–6542 (2014).
135. Sun, Y. *et al.* Fabrication of mPEGylated graphene oxide/poly(2-dimethyl aminoethyl methacrylate) nanohybrids and their primary application for small interfering RNA delivery. *J. Appl. Polym. Sci.* **133,** (2016).
136. Choi, H. Y. *et al.* Efficient mRNA delivery with graphene oxide-polyethylenimine for generation of footprint-free human induced pluripotent stem cells. *J. Control. Release* **235,** 222–235 (2016).
137. Shen, H. *et al.* PEGylated graphene oxide-mediated protein delivery for cell function regulation. *ACS Appl. Mater. Interfaces* **4,** 6317–6323 (2012).
138. Choi, M. *et al.* Multilayered Graphene Nano-Film for Controlled Protein Delivery by Desired Electro-Stimuli. *Sci. Rep.* **5,** (2015).
139. La, W. G. *et al.* Delivery of a therapeutic protein for bone regeneration from a substrate coated with graphene oxide. *Small* **9,** 4051–4060 (2013).
140. Li, H. *et al.* Spontaneous Protein Adsorption on Graphene Oxide Nanosheets Allowing Efficient Intracellular Vaccine Protein Delivery. *ACS Appl. Mater. Interfaces* **8,** 1147–1155 (2016).
141. Kaur, J. & Debnath, J. Autophagy at the crossroads of catabolism and anabolism. *Nature Reviews Molecular Cell Biology* **16,** 461–472 (2015).
142. Mizushima, N. & Klionsky, D. J. Protein Turnover Via Autophagy: Implications for Metabolism. *Annu. Rev. Nutr.* **27,** 19–40 (2007).
143. Gatica, D., Lahiri, V. & Klionsky, D. J. Cargo recognition and degradation by selective autophagy. *Nat. Cell Biol.* **20,** 233–242 (2018).
144. Eskelinen, E.-L., Reggiori, F., Baba, M., Kovács, A. L. & Seglen, P. O. Seeing is believing: The impact of electron microscopy on autophagy research. *Autophagy* **7,** 935–956 (2011).
145. Galluzzi, L., Bravo-San Pedro, J. M., Levine, B., Green, D. R. & Kroemer, G. Pharmacological modulation of autophagy: therapeutic potential and persisting obstacles. *Nat. Rev. Drug Discov.* **16,** 487 (2017).
146. Feng, Y., He, D., Yao, Z. & Klionsky, D. J. The machinery of

macroautophagy. *Cell Research* **24,** 24–41 (2014).
147. Gomes, L. R., Menck, C. F. M. & Cuervo, A. M. Chaperone-mediated autophagy prevents cellular transformation by regulating MYC proteasomal degradation. *Autophagy* **13,** 928–940 (2017).
148. Towers, C. G. & Thorburn, A. Therapeutic Targeting of Autophagy. *EBioMedicine* **14,** 15–23 (2016).
149. Rubinsztein, D. C., Codogno, P. & Levine, B. Autophagy modulation as a potential therapeutic target for diverse diseases. *Nature Reviews Drug Discovery* **11,** 709–730 (2012).
150. Füllgrabe, J., Klionsky, D. J. & Joseph, B. The return of the nucleus: Transcriptional and epigenetic control of autophagy. *Nature Reviews Molecular Cell Biology* **15,** 65–74 (2014).
151. Amaravadi, R. K. Transcriptional regulation of autophagy in RAS-driven cancers. *Journal of Clinical Investigation* **125,** 1393–1395 (2015).
152. Konstantinidis, G., Sievers, S. & Wu, Y.-W. Identification of Novel Autophagy Inhibitors via Cell-Based High-Content Screening. in *Methods in molecular biology (Clifton, N.J.)* (2018). doi:10.1007/7651_2018_125
153. Robke, L. *et al.* Phenotypic Identification of a Novel Autophagy Inhibitor Chemotype Targeting Lipid Kinase VPS34. *Angew. Chemie - Int. Ed.* **56,** 8153–8157 (2017).
154. Laraia, L. *et al.* Discovery of Novel Cinchona-Alkaloid-Inspired Oxazatwistane Autophagy Inhibitors. *Angew. Chemie - Int. Ed.* **56,** 2145–2150 (2017).
155. Arias, E. *et al.* Lysosomal mTORC2/PHLPP1/Akt Regulate Chaperone-Mediated Autophagy. *Mol. Cell* **59,** 270–284 (2015).
156. Sarkar, S., Davies, J. E., Huang, Z., Tunnacliffe, A. & Rubinsztein, D. C. Trehalose, a novel mTOR-independent autophagy enhancer, accelerates the clearance of mutant huntingtin and α-synuclein. *J. Biol. Chem.* **282,** 5641–5652 (2007).
157. DeBosch, B. J. *et al.* Trehalose inhibits solute carrier 2A (SLC2A) proteins to induce autophagy and prevent hepatic steatosis. *Sci. Signal.* **9,** (2016).
158. Egan, D. F. *et al.* Small Molecule Inhibition of the Autophagy Kinase ULK1 and Identification of ULK1 Substrates. *Mol. Cell* **59,** 285–297 (2015).
159. Marsh, T. & Debnath, J. Ironing out VPS34 inhibition. *Nature Cell Biology* **17,** 1–3 (2015).

160. Sinha, S. & Levine, B. The autophagy effector Beclin 1: A novel BH3-only protein. *Oncogene* **27,** S137–S148 (2008).
161. Maiuri, M. C. *et al.* Functional and physical interaction between Bcl-XL and a BH3-like domain in Beclin-1. *EMBO J.* **26,** 2527–2539 (2007).
162. Reljic, B. *et al.* BAX-BAK1-independent LC3B lipidation by BH3 mimetics is unrelated to BH3 mimetic activity and has only minimal effects on autophagic flux. *Autophagy* **12,** 1083–1093 (2016).
163. Shoji-Kawata, S. *et al.* Identification of a candidate therapeutic autophagy-inducing peptide. *Nature* **494,** 201–206 (2013).
164. Levine, B., Packer, M. & Codogno, P. Development of autophagy inducers in clinical medicine. *Journal of Clinical Investigation* **125,** 14–24 (2015).
165. He, C. *et al.* Exercise-induced BCL2-regulated autophagy is required for muscle glucose homeostasis. *Nature* **481,** 511–515 (2012).
166. Akin, D. *et al.* A novel ATG4B antagonist inhibits autophagy and has a negative impact on osteosarcoma tumors. *Autophagy* **10,** 2021–2035 (2014).
167. Itakura, E., Kishi-Itakura, C. & Mizushima, N. The hairpin-type tail-anchored SNARE syntaxin 17 targets to autophagosomes for fusion with endosomes/lysosomes. *Cell* **151,** 1256–1269 (2012).
168. Geim, A. K. & Novoselov, K. S. The rise of graphene. *Nat. Mater*. **6,** 183–191 (2007).
169. Muratov, E. N. *et al.* Per aspera ad astra: application of Simplex QSAR approach in antiviral research. *Future Med. Chem.* **2,** 1205–26 (2010).
170. Chen, B., Zhang, T., Bond, T. & Gan, Y. Development of quantitative structure activity relationship (QSAR) model for disinfection byproduct (DBP) research: A review of methods and resources. *Journal of Hazardous Materials* **299,** 260–279 (2015).
171. Merrifield, R. B. Solid Phase Peptide Synthesis. I. The Synthesis of Tetrapeptide. *J. Am. Chem. Soc.* **85,** 2149–2154 (1963).
172. Lin, P. C., Lin, S., Wang, P. C. & Sridhar, R. Techniques for physicochemical characterization of nanomaterials. *Biotechnology Advances* **32,** 711–726 (2014).
173. Lambert, L. & Mulvey, T. Ernst Ruska (1906–1988), Designer Extraordinaire of the Electron Microscope: A Memoir. *Adv. Imaging Electron Phys.* **95,** 2–62 (1996).
174. Winston, P. H. Marvin L. Minsky (1927-2016). *Nature* **530,** 282

(2016).
175. Douglas, J. HeLa. *Nature* **242,** 543 (1973).
176. Kang, S. H., Cho, M. J. & Kole, R. Up-regulation of luciferase gene expression with antisense oligonucleotides: implications and applications in functional assay development. *Biochemistry* **37,** 6235–6239 (1998).
177. Graham, F. L., Smiley, J., Russell, W. C. & Nairn, R. Characteristics of a human cell line transformed by DNA from human adenovirus type 5. *J. Gen. Virol.* **36,** 59–74 (1977).
178. Greer, L. F. & Szalay, A. A. Imaging of light emission from the expression of luciferases in living cells and organisms: A review. *Luminescence* **17,** 43–47 (2002).
179. Naylor, L. H. Reporter gene technology: the future looks bright. *Biochem. Pharmacol.* **58,** 749–757 (1999).
180. Ryan, M. M. *et al.* Application and optimization of microarray technologies for human postmortem brain studies. *Biological Psychiatry* **55,** 329–336 (2004).
181. Lee, C. T. *et al.* Cocaine promotes primary human astrocyte proliferation via JNK-dependent up-regulation of cyclin A2. *Restor. Neurol. Neurosci.* **34,** 965–976 (2016).
182. Okoniewski, M. J. & Miller, C. J. Hybridization interactions between probesets in short oligo microarrays lead to spurious correlations. *BMC Bioinformatics* **7,** 276 (2006).
183. Shendure, J. The beginning of the end for microarrays? *Nat. Methods* **5,** 585–587 (2008).
184. Wang, Z., Gerstein, M. & Snyder, M. RNA-Seq: A revolutionary tool for transcriptomics. *Nature Reviews Genetics* **10,** 57–63 (2009).
185. Dowaidar, M. *et al.* Magnetic Nanoparticle Assisted Self-assembly of Cell Penetrating Peptides-Oligonucleotides Complexes for Gene Delivery. *Sci. Rep.* **7,** 9159 (2017).
186. Regberg, J. *et al.* Rational design of a series of novel amphipathic cell-penetrating peptides. *Int. J. Pharm.* **464,** 111–116 (2014).
187. Wilhelm, S. *et al.* Analysis of nanoparticle delivery to tumours. *Nature Reviews Materials* **1,** (2016).
188. Ezzat, K. *et al.* Scavenger receptor-mediated uptake of cell-penetrating peptide nanocomplexes with oligonucleotides. *FASEB J.* **26,** 1172–1180 (2012).
189. Nair, B. G., Fukuda, T., Mizuki, T., Hanajiri, T. & Maekawa, T. Intracellular trafficking of superparamagnetic iron oxide nanoparticles conjugated with TAT peptide: 3-dimensional

electron tomography analysis. *Biochem. Biophys. Res. Commun.* **421,** 763–767 (2012).
190. Yang, Y. *et al.* Thermal and magnetic dual-responsive liposomes with a cell-penetrating peptide-siRNA conjugate for enhanced and targeted cancer therapy. *Colloids Surfaces B Biointerfaces* **146,** 607–615 (2016).
191. Min, S. K., Kim, W. Y., Cho, Y. & Kim, K. S. Fast DNA sequencing with a graphene-based nanochannel device. *Nat. Nanotechnol.* **6,** 162–165 (2011).
192. Li, Q. *et al.* Modulating Aβ 33-42 Peptide Assembly by Graphene Oxide. *Chem. - A Eur. J.* **20,** 7236–7240 (2014).
193. Lindberg, S. *et al.* A convergent uptake route for peptide- and polymer-based nucleotide delivery systems. *J. Control. Release* **206,** 58–66 (2015).
194. Wei, Y., Zhou, F., Zhang, D., Chen, Q. & Xing, D. A graphene oxide based smart drug delivery system for tumor mitochondria-targeting photodynamic therapy. *Nanoscale* **2016,** 3530–3538 (2016).
195. Dowaidar, M. *et al.* Role of autophagy in cell-penetrating peptide transfection model. *Sci. Rep.* **7,** (2017).
196. Hamilton, R. F., Thakur, S. A., Mayfair, J. K. & Holian, A. MARCO mediates silica uptake and toxicity in alveolar macrophages from C57BL/6 mice. *J. Biol. Chem.* **281,** 34218–34226 (2006).
197. Allison, A. C. An examination of the cytotoxic effects of silica on macrophages. *J. Exp. Med.* **124,** 141–154 (1966).
198. Stern, S. T., Adiseshaiah, P. P. & Crist, R. M. Autophagy and lysosomal dysfunction as emerging mechanisms of nanomaterial toxicity. *Part. Fibre Toxicol.* **9,** 20 (2012).
199. Davis, M. E. *et al.* Evidence of RNAi in humans from systemically administered siRNA via targeted nanoparticles. *Nature* **464,** 1067–1070 (2010).
200. Herd, H. L., Malugin, A. & Ghandehari, H. Silica nanoconstruct cellular toleration threshold in vitro. in *Journal of Controlled Release* **153,** 40–48 (2011).
201. Khan, M. I. *et al.* Induction of ROS, mitochondrial damage and autophagy in lung epithelial cancer cells by iron oxide nanoparticles. *Biomaterials* **33,** 1477–1488 (2012).
202. Pérez-Carriõn, M. D. *et al.* Dendrimer-mediated siRNA delivery knocks down Beclin 1 and potentiates NMDA-mediated toxicity in rat cortical neurons. *J. Neurochem.* **120,** 259–268 (2012).

203. Vernon, P. J. & Tang, D. Eat-Me: Autophagy, Phagocytosis, and Reactive Oxygen Species Signaling. *Antioxid. Redox Signal.* **18,** 677–691 (2013).
204. Roberts, R. *et al.* Autophagy and formation of tubulovesicular autophagosomes provide a barrier against nonviral gene delivery. *Autophagy* **9,** 667–682 (2013).
205. Kaushik, S. & Cuervo, A. M. Chaperone-mediated autophagy: A unique way to enter the lysosome world. *Trends in Cell Biology* **22,** 407–417 (2012).
206. Agarraberes, F. a & Dice, J. F. A molecular chaperone complex at the lysosomal membrane is required for protein translocation. *J. Cell Sci.* **114,** 2491–2499 (2001).
207. Budina-Kolomets, A. *et al.* Comparison of the activity of three different HSP70 inhibitors on apoptosis, cell cycle arrest, autophagy inhibition, and HSP90 inhibition. *Cancer Biol. Ther.* **15,** 194–199 (2014).
208. Owen, K. A., Meyer, C. B., Bouton, A. H. & Casanova, J. E. Activation of Focal Adhesion Kinase by Salmonella Suppresses Autophagy via an Akt/mTOR Signaling Pathway and Promotes Bacterial Survival in Macrophages. *PLoS Pathog.* **10,** e1004159 (2014).
209. Chiu, H.-W. *et al.* Cationic polystyrene nanospheres induce autophagic cell death through the induction of endoplasmic reticulum stress. *Nanoscale* **7,** 736–46 (2014).
210. Farah, B. L. *et al.* β-adrenergic agonist and antagonist regulation of autophagy in HepG2 cells, primary mouse hepatocytes, and mouse liver. *PLoS One* **9,** (2014).
211. Gao, S. *et al.* Atorvastatin activates autophagy and promotes neurological function recovery after spinal cord injury. *Neural Regen. Res.* **11,** 0 (2016).
212. Chen, H., Chen, L., Cheng, B. & Jiang, C. Cyclic mechanical stretching induces autophagic cell death in tenofibroblasts through activation of prostaglandin E2 production. *Cell. Physiol. Biochem.* **36,** 24–33 (2015).